development [10-15]. Indeed, HDAC inhibitors such as suberoylanilide hydroxamic acid (SAHA) **1** [16] and NVP-LAQ824 **2** [17] (Fig. (**2**)) are currently in clinical trials for the treatment of cancer.

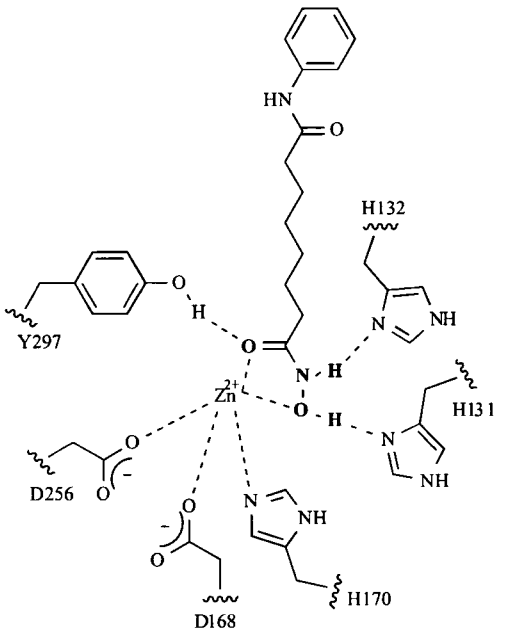

Fig. (3). SAHA in the catalytic core of HDLP.

Research potential in the development of HDAC inhibitors accelerated when the X-ray crystal structures of an archaebacterial HDAC homologue (HDAC-like protein, HDLP)/hydroxamic acid inhibitors were disclosed [18]. The structures made it clear that the enzyme contains a zinc ion at the bottom of the active site and that the hydroxamic acid group coordinates the zinc ion through its CO and OH groups and also forms three hydrogen bonds between its CO, NH and OH groups and Tyr 297, His 132 and His 131, respectively (Fig. (**3**)). The crystal structures have led to a solid understanding of not only the three-dimensional structure of the active site of HDACs but also the catalytic mechanism for the deacetylation of acetylated lysine substrate. It has been proposed that the carbonyl oxygen of the substrate could bind the zinc ion, and the carbonyl could be attacked by a zinc-chelating water molecule, which would result in the production of deacetylated lysine via a tetrahedral carbon-containing transition state (Fig. (**4**)). The crystal structures of human HDAC8 complexed with hydroxamates, reported recently [19, 20], also supported such a catalytic mechanism of HDACs.

To date, a number of HDAC inhibitors have been developed. As depicted in Fig. (**5**), HDAC inhibitors typically possess a zinc-binding group (ZBG), which coordinates the zinc ion in the active site, a cap substructure, which interacts with amino acids at the entrance of the *N*-acetylated lysine binding channel, and a linker connecting the cap and the ZBG at a proper distance. Most of the previously reported HDAC inhibitors are hydroxamic acid derivatives, typified by SAHA **1**, NVP-LAQ824 **2** and Trichostatin A (TSA) **3** [21, 22] (Fig. (**2**)), which are thought to chelate the zinc ion in the active site in a bidentate fashion through its CO and OH groups [18-20]. Although hydroxamic acids are frequently employed as ZBGs, they often present metabolic and pharmacokinetic problems such as glucoronidation and sulfation that result in a short *in vivo* half-life [23, 24]. Indeed, it has been reported that intravenous administration of SAHA **1** has a half-life ranging from 21 to 58 min in patients [25]. TSA **3** has been reported to have no antitumor activity in nude mice bearing xenografts of human melanoma cells [26], which is probably

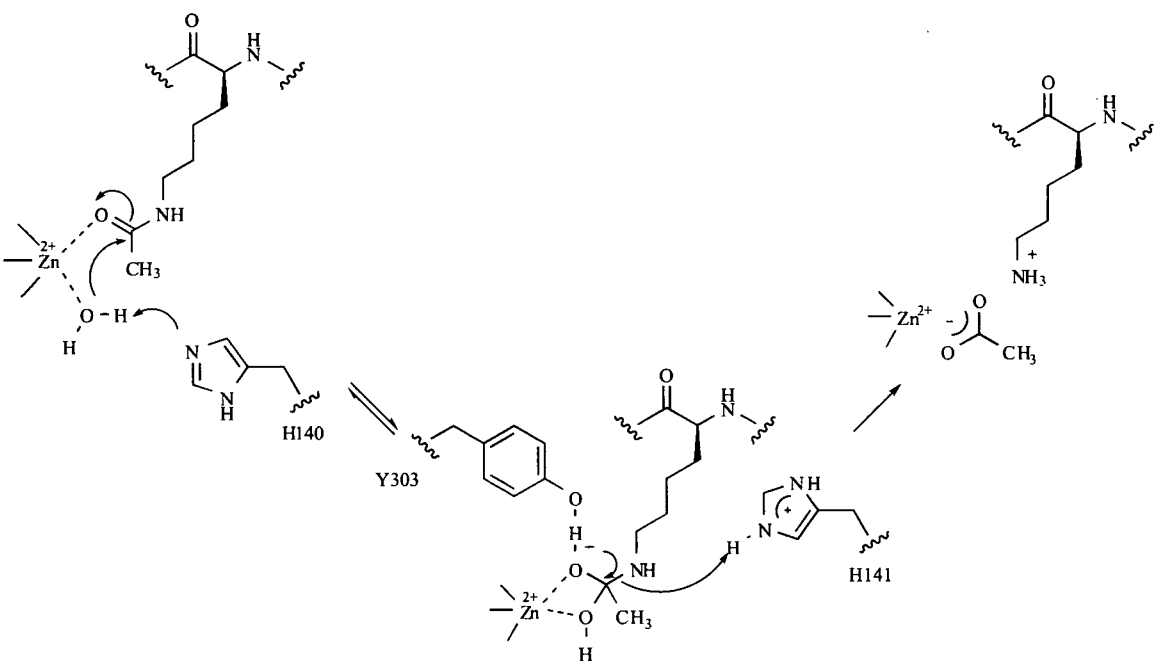

Fig. (4). Proposed catalytic mechanism for the deacetylation of acetylated lysine.

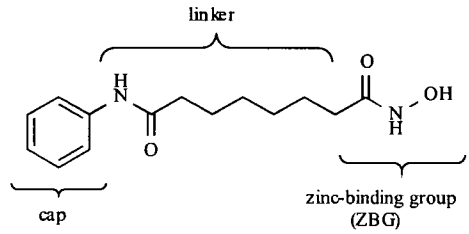

Fig. (5). Pharmacophoric summary of the structural characteristics of HDAC inhibitors.

a consequence of metabolic inactivation of TSA **3**. Furthermore, many hydroxamates are unstable in vivo, and are prone to hydrolysis giving hydroxylamine which has potential mutagenic properties [27]. In addition, although isozyme-selective HDAC inhibitors are considered useful not only as tools for probing the biology of an enzyme but as drugs with low toxicity, hydroxamate HDAC inhibitors, with the exception of a few compounds such as tubacin [28] and (3-fluorophenyloxopropenyl)pyrrolyl hydroxamate [29], do not distinguish well among the HDAC isozymes. Thus, there has been considerable interest in developing non-hydroxamate HDAC inhibitors. Many groups have ongoing research programs to find non-hydroxamate inhibitors of HDACs, and these efforts have led to the identification of several classes of inhibitors. In this review, we introduce non-hydroxamate HDAC inhibitors describing their design, enzyme inhibition, cancer cell growth inhibition and isozyme selectivity.

NON-HYDROXAMATE INHIBITORS OF HISTONE DEACETYLASES

Small Fatty Acids

Sodium butyrate **4** (Fig. (**6**)) has long been known to have antiproliferative and differentiating activity against several types of cancer cells [30]. It was later revealed that **4** inhibits HDACs at high micromolar concentrations, which explains the anticancer mechanism of **4** [31]. Most probably, **4** inhibits HDACs by binding to their catalytic center.

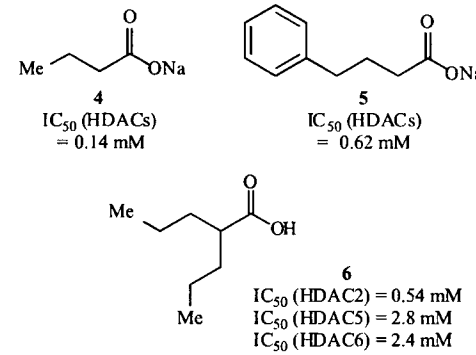

Fig. (6). Small fatty acid HDAC inhibitors.

To date, several short-chain fatty acid analogues of **4**, such as sodium phenylbutyrate **5** and valproic acid **6**, have also been reported to show inhibition of HDACs and antiproliferative activity, although their inhibitory activity is weak (IC_{50} > 0.1 mM) [32-34]. Nevertheless, it is noteworthy that a combination of **5** and all-trans retinoic acid induced histone hyperacetylation and complete remission of a highly resistant promyelocytic leukemia without severe side effects in a patient [35]. In addition, it has also been reported that tumor metastasis was significantly reduced by valproic acid **6** in animal experiments [32]. Some of the small fatty acid analogues such as **4** and **6** are currently in Phase I or Phase I/II trials for the treatment of cancer [36].

Epoxyketones

Cyclic tetrapeptides bearing epoxyketone such as HC-toxin I **7** and trapoxin B **8** (Fig. (**7**)) were originally discovered by screening natural products for antiparasitic or

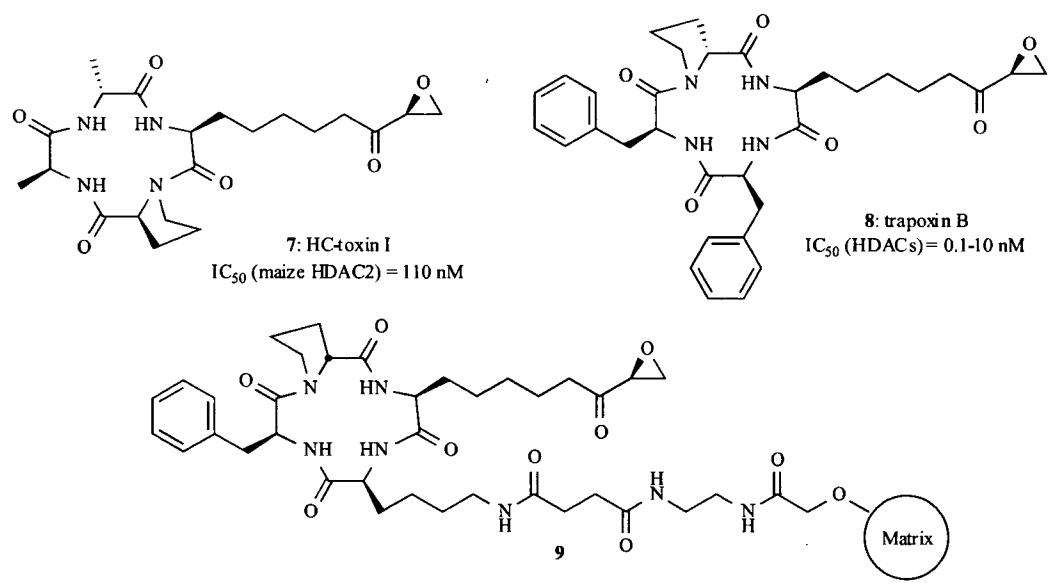

Fig. (7). HDAC inhibitors with epoxyketone.

antiproliferative activity [37-41]. These compounds were also identified as HDAC inhibitors [42-44]. Experiments in vitro using mouse histone deacetylase revealed that a low concentration of **8** irreversibly inhibits the deacetylation of acetylated histones [42]. It is easily speculated that the epoxide of **8** is attacked by an active site nucleophile such as histidine. Applying trapoxin B's characteristic irreversible inhibition of HDAC activity, the isolation and cloning of a human HDAC were achieved. Trapoxin B affinity matrix **9** was used to isolate a novel nuclear protein HD1 (HDAC1) using affinity chromatography [4].

Although the epoxyketone moiety seems essential for inhibitory activity, several cyclic tetrapeptides without the epoxyketone structure inhibited HDACs as well [45-47]. Furthermore, HC-toxin I **7** was found to inhibit maize HDAC reversibly and non-competitively with acetylated lysine substrate [43]. It remains unclear whether the covalent bond formed *via* the reaction of the epoxyketone with a nucleophile at the active site is responsible for the inhibitory activity.

o-Aminoanilides

Suzuki and co-workers identified MS-275 **10** (Fig. (**8**)) from a set of synthetic benzamide derivatives [48]. MS-275 **10** inhibited HDACs with an IC_{50} of 4.8 μM and showed significant oral anticancer activity without severe side effects in animal models [49]. MS-275 **10** is currently in phase II clinical trials for the treatment of cancer. CI-994 **11**, another *o*-aminoanilide compound from Pfizer which is in phase II clinical trials, was recently found to inhibit HDAC1 and HDAC2 without affecting the activity of the prototypical histone acetyltransferase GCN5 [50]. Sulfonamide anilides such as MGCD0103 **12** were identified as inhibitors of HDACs [51, 52]. Compound **12** exhibited antitumor activity in vitro and in vivo. The antitumor activity of **12** correlated well with its ability to arrest the cell cycle and to alter the expression of cell cycle regulators such as $p21^{WAF1/CIP1}$ and cyclin A. MGCD0103 **12** is presently entered into phase I clinical trials for the treatment of cancer. A series of ω-substituted alkanoic acid (2-aminophenyl)amides such as **13** have been reported recently [53, 54]. These compounds inhibited recombinant human HDAC1 with IC_{50} values ranging from 0.5 to 12 μM. Compound **13** showed efficacy in human tumor xenograft models. However, the activity was lower than that of MS-275 **10**. Schreiber and co-workers synthesized about 2,400 *o*-aminoanilides using the combinatorial approach to find isozyme-selective HDAC inhibitors [55]. This approach led to the identification of histacin **14** and the related compound PAOA **15**, inhibitors inactive toward HDAC6 in cells [28, 56] (see the section Isozyme Selectivity).

As mentioned above, it has been clearly demonstrated that several *o*-aminoanilides possess antitumor activity that is associated with HDAC inhibitory activity. At present, it is yet unclear whether *o*-aminoanilide derivatives interact

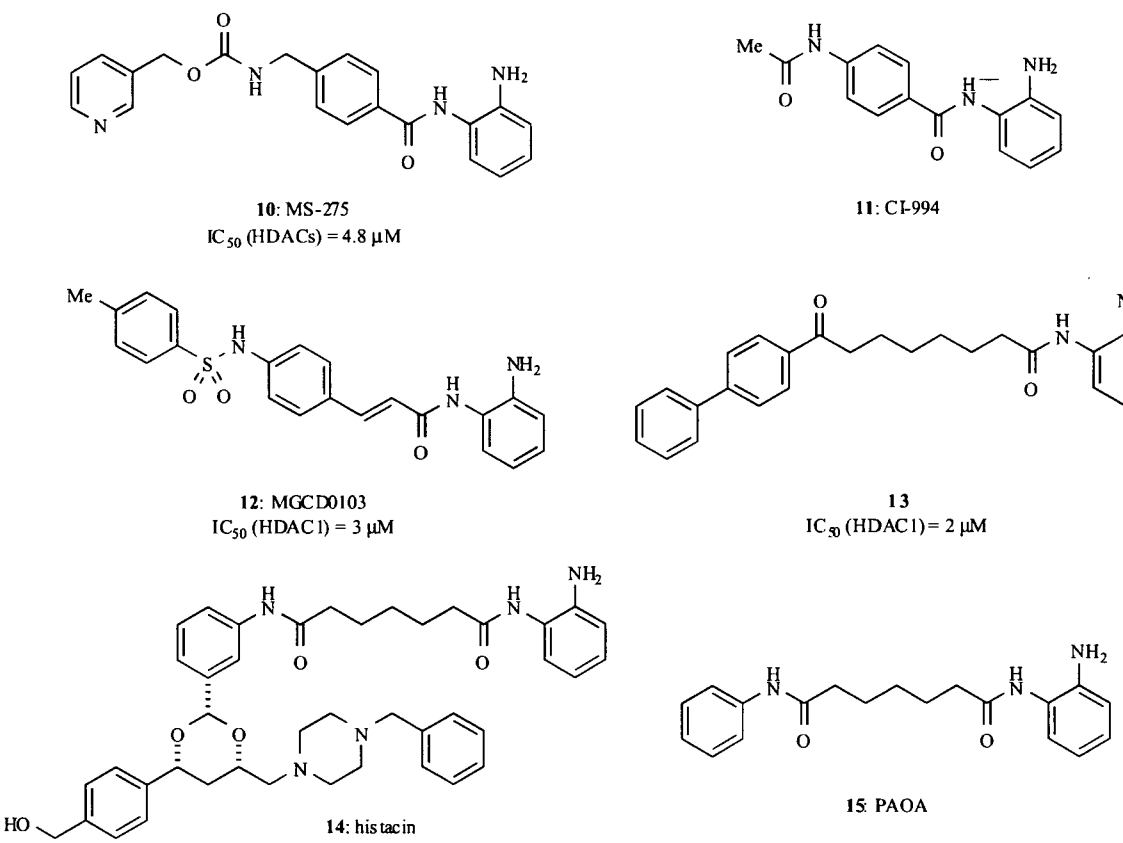

Fig. (8). HDAC inhibitors with *o*-aminoanilide.

with the zinc ion and amino acid residues in the active site or bind at an allosteric site. However, the similar structure-activity relationship between *o*-aminoanilides and hydroxamates indicates that *o*-aminoanilides inhibit HDACs in a binding mode similar to hydroxamates [51, 53, 54, 57].

Electrophilic Ketones

Electrophilic ketones have been a fruitful area of investigation in the search for novel HDAC inhibitors [58]. As shown in Fig. (**9**), electrophilic ketones are readily hydrated to form 1,1-diols which could coordinate zinc ion

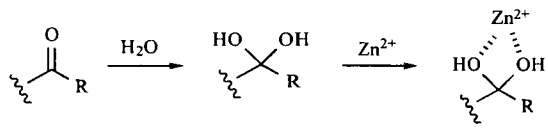

Fig. (9). Inhibition of HDACs by electrophilic ketones.

in the active site of HDACs. Frey and co-workers at Abbott reported trifluoromethyl ketones as HDAC inhibitors [59]. Trifluoromethyl ketones such as **16** (Fig. (**10**)) showed inhibitory activity against a mixture of HDAC1 and HDAC2 (IC_{50} of **16** = 0.38 μM). Compound **16** demonstrated antiproliferative effects against HT1080 and MDA435 cell lines and induced histone H4 hyperacetylation and $p21^{WAF1/CIP1}$ expression in MDA435 cells. Nishino and co-workers prepared cyclic tetrapeptide with trifluoromethyl and pentafluoroethyl ketones [60]. Compound **17** showed potent activity in a human HDAC inhibition assay and p21 promoter assay. Other reported structures of electrophilic ketone inhibitors include α-ketoamides and heterocyclic ketones such as **18**, **19** and **20** [61-63]. Notably, α-ketoamides showed potent inhibition of HDAC (IC_{50} < 10 nM) and excellent antiproliferative activity against HT1080 and MDA435 cell lines (IC_{50} < 1 μM). This class of inhibitors have a metabolic problem in that they are readily reduced to the corresponding alcohols in vivo, even within cells. Nevertheless, compound **18** exhibited significant antitumor effects in an in vivo tumor model. These results suggest that a brief exposure to HDAC inhibitors can produce in vivo biological activity.

N-Formyl Hydroxylamines

The crystal structures of HDLP/hydroxamate and HDAC8/hydroxamate complexes made it clear that the

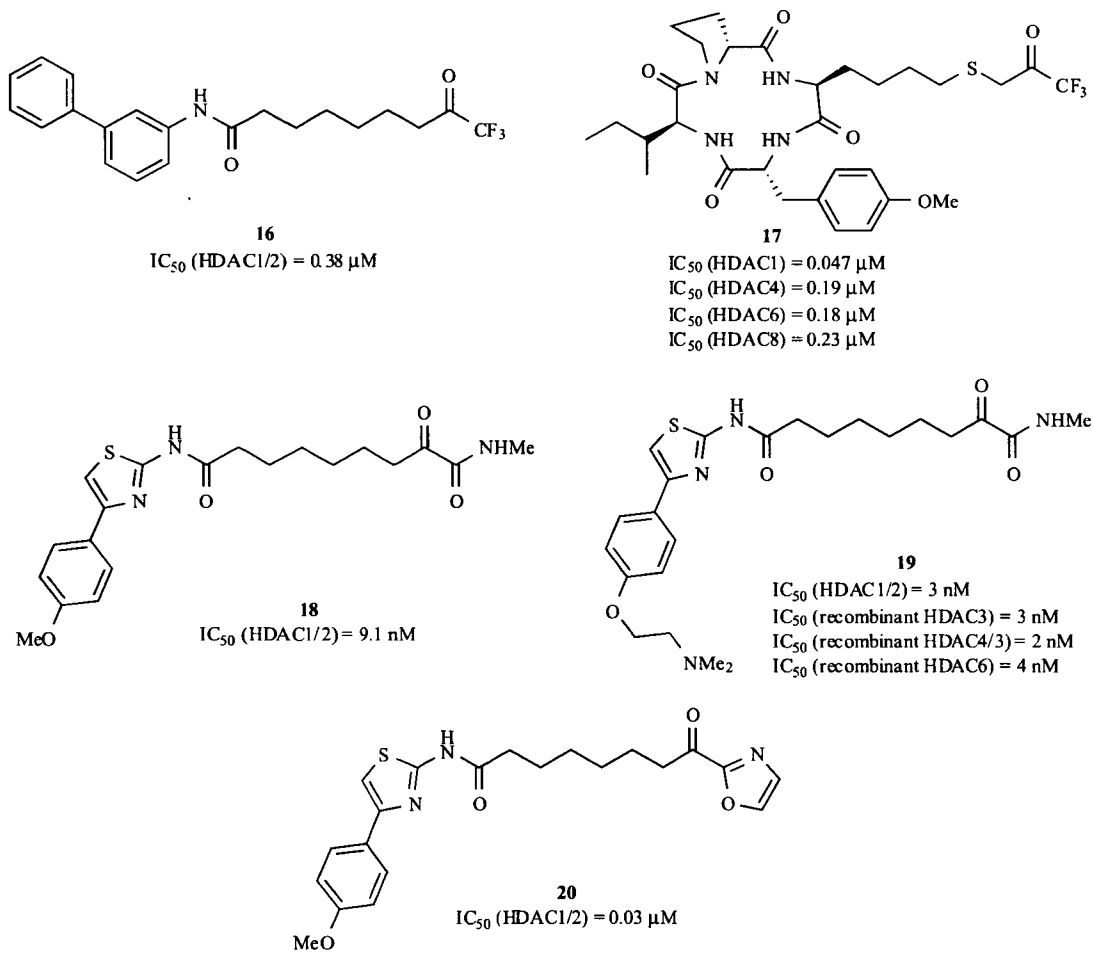

Fig. (10). HDAC inhibitors with electrophilic ketones.

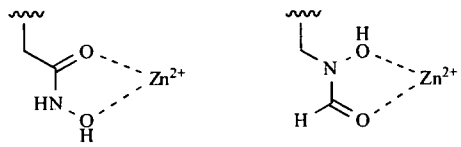

Fig. (11). Model for the binding of hydroxamic acid (left) and *N*-formylhydroxylamine (right) to zinc ion.

hydroxamic acid group coordinates the zinc ion in the active site through its CO and OH groups (Fig. (**3**); Fig. (**11**), left) [18-20]. Compounds bearing *N*-formyl hydroxylamine could inhibit HDACs by forming a bidentate chelate with zinc ion (Fig. (**11**), right). Schultz and co-workers synthesized a series of *N*-formyl hydroxylamines and evaluated their biological activity [64]. Among these compounds, compound **21** (Fig. (**12**)) displayed HDAC inhibitory

Thiols

Thiols are an attractive ZBG for incorporation in HDAC inhibitors, because zinc ion is highly thiophilic and thiol derivatives have been reported to inhibit zinc-dependent enzymes such as angiotensin converting enzyme [66] and matrix metalloproteinases [27]. We found that compound **23** (Fig. (**13**)), in which the hydroxamic acid of SAHA **1** is replaced by a thiol, was as potent as SAHA **1** in an enzyme assay using HeLa nuclear extracts (IC_{50} of SAHA **1** = 0.28 μM, IC_{50} of **23** = 0.21 μM) [67]. The results of an enzyme kinetic assay (Lineweaver-Burk plot) established that thiol **23** engages in competitive inhibition versus acetylated lysine substrate, with an inhibition constant (*Ki*) of 0.11 μM [68]. Optimization of the linker part and aromatic cap part of **23** led to the identification of HDAC inhibitors such as **24** and **25**, which are more potent than SAHA **1** in enzyme assays.

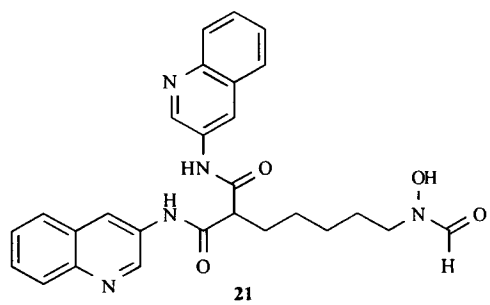

21
IC_{50} (HDAC1) = 0.16 μM
IC_{50} (HDAC2) = 0.20 μM
IC_{50} (HDAC6) = 0.78 μM
IC_{50} (HDAC8) = 0.69 μM
IC_{50} (HDACs) = 0.97 μM

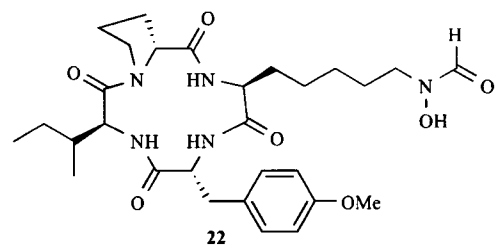

22
IC_{50} (HDAC1) = 0.033 μM
IC_{50} (HDAC4) = 0.089 μM
IC_{50} (HDAC6) = 0.029 μM
IC_{50} (HDAC8) = 0.034 μM

Fig. (12). HDAC inhibitors with *N*-formylhydroxylamine.

activity in the submicromolar range. The antiproliferative activity of compound **21** was comparable to that of SAHA **1**. Nishino and co-workers presented cyclic tetrapeptides having *N*-formyl hydroxylamine as HDAC inhibitors [65]. Cyclic tetrapeptides such as **22** were 10 times more potent than straight chain *N*-formyl hydroxylamines such as **21**.

Although compound **23** was weakly active in a cell growth inhibition assay with NCI-H460 cells (34% inhibition at 50 μM), the prodrug approach improved the antiproliferative activity [68]. *S*-Isobutyryl compound **26**, a prodrug of **23**, inhibited the growth of NCI-H460 cells with an EC_{50} of 20 μM. Furthermore, optimization of the cap part of **26** to

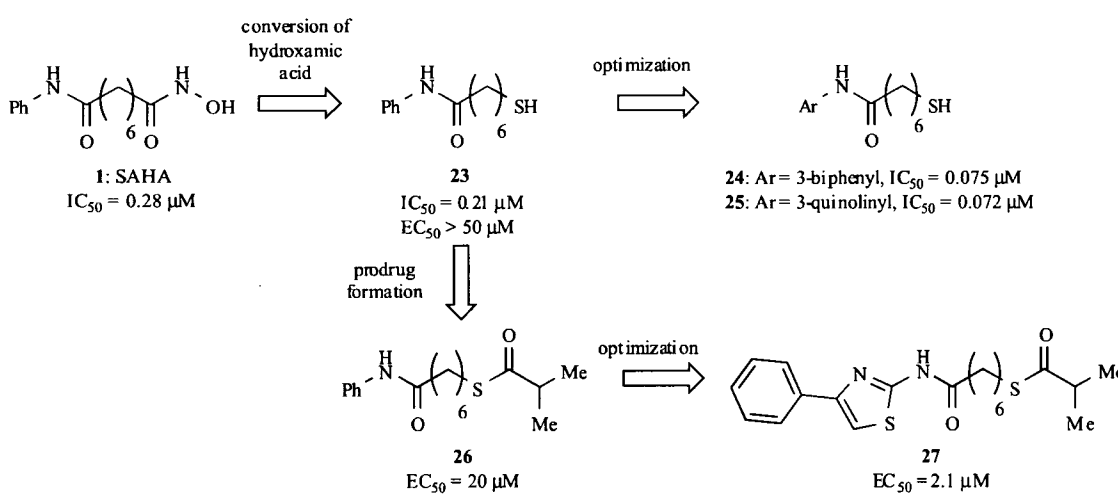

1: SAHA
IC_{50} = 0.28 μM

23
IC_{50} = 0.21 μM
EC_{50} > 50 μM

24: Ar = 3-biphenyl, IC_{50} = 0.075 μM
25: Ar = 3-quinolinyl, IC_{50} = 0.072 μM

26
EC_{50} = 20 μM

27
EC_{50} = 2.1 μM

Fig. (13). Thiol-based HDAC inhibitors. IC_{50}: Inhibitory activity against human HDACs; EC_{50}: antiproliferative activity.

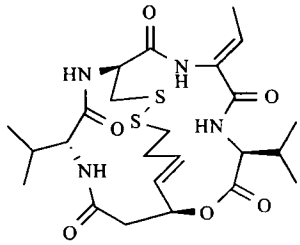

28: FK228
IC_{50} (HDAC1) = 36 nM
IC_{50} (HDAC1) = 1 nM (reductive condition)

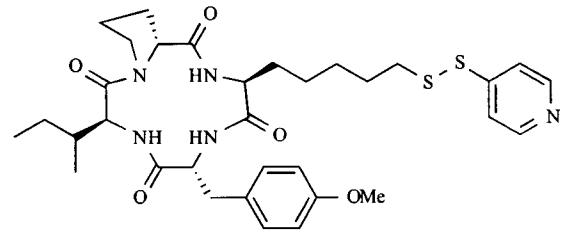

29
IC_{50} (HDAC1) = 7 nM
IC_{50} (HDAC1) = 0.55 nM (reductive condition)

Fig. (14). HDAC inhibitors with disulfide.

various aromatic rings led to a highly potent cancer cell growth inhibitor **27**. Compound **27** exerted potent antiproliferative activity against various human cancer cells, with EC_{50} values ranging from 1 to 10 μM, and these activities were comparable to those of SAHA **1** (average EC_{50} of **27** 3.8 μM, SAHA **1** 3.7 μM) which is currently being evaluated in clinical trials for use in the treatment of cancer. In addition, treatment of HCT 116 cells with compound **27** gave rise to elevated and dose-dependent levels of acetylated histone H4 and $p21^{WAF1/CIP1}$. These results suggested that the antiproliferative activity of compound **27** significantly correlates with the inhibition of intracellular HDACs.

Furumai and co-workers demonstrated that the disulfide bond of FK228 **28** (Fig. (**14**)), a depsipeptide HDAC inhibitor, is reduced in the cellular environment, releasing the free thiol analogue as the active species [69], and Nishino and co-workers reported that cyclic tetrapeptides bearing a disulfide group such as **29** inhibit HDACs potently under reductive conditions [70].

Modeling of compound **23** docked with HDAC8 suggested that the thiol of compound **23** interacts directly with the zinc ion in the active site of HDACs [68] (Fig. (**15**), left), whereas computer modeling of reduced FK228 suggests that the thiol of the reduced FK228 interacts with the zinc ion via a water molecule [69] (Fig. (**15**), right).

Mercaptoamides

We identified a mercaptoacetamide-based inhibitor **30** (Fig. (**16**)) by mechanism-based drug design [71]. On the basis of the proposed catalytic mechanism (Fig. (**17**)a), the HDACs would supposedly be inhibited if the water molecule is forcibly removed from the zinc ion, and then heteroatom-containing substrate analogues **30**, **31** and **32** were designed and synthesized (Fig. (**16**)). These analogues would be recognized as substrates by HDACs and be easily taken into the active site where they force the water molecule off the zinc ion and the reactive site for the deacetylation by chelation of the heteroatom to the zinc ion, and behave as

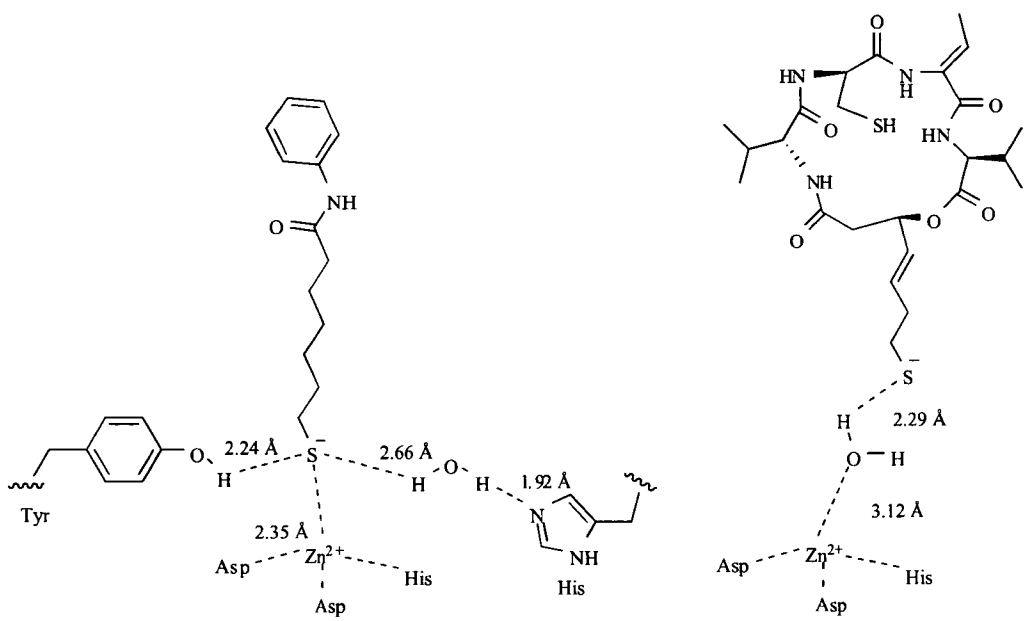

Fig. (15). Low energy conformation of **23** docked in the HDAC8 catalytic core (left) and of reduced FK228 in the HDLP catalytic core (right).

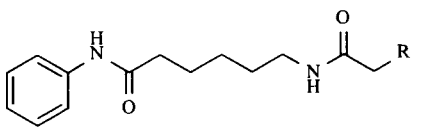

30: R = -SH, IC_{50} (HDACs) = 0.39 μM
31: R = -OH, IC_{50} (HDACs) > 100 μM
32: R = $-NH_2$, IC_{50} (HDACs) > 100 μM

Fig. (16). Hetero atom-containing substrate analogues designed on the basis of the deacetylation mechanism.

HDAC inhibitors (Fig. (**17**)b). As we had expected, strong inhibition was observed with mercaptoacetamide **30**, while lysine substrate, with an inhibition constant (Ki) of 0.78 μM on Lineweaver-Burk plots. The low energy conformation of **30** docked in the model based on the crystal structure of HDAC8 was calculated. An inspection of the HDAC8/**30** complex showed that the sulfur atom and oxygen atom of **30** were located 2.44 Å and 2.04 Å from the zinc ion, respectively, and that a water molecule, which is required for the deacetylation of acetylated lysine substrate, was positioned 4.95 Å apart from the zinc ion (Fig. (**18**)). This calculation suggests that **30** inhibits HDACs by chelating the zinc ion in a bidentate fashion through its sulfur and oxygen atoms, and by removing a water molecule from the zinc and the reactive site of the deacetylation, without being hydrolyzed by HDACs.

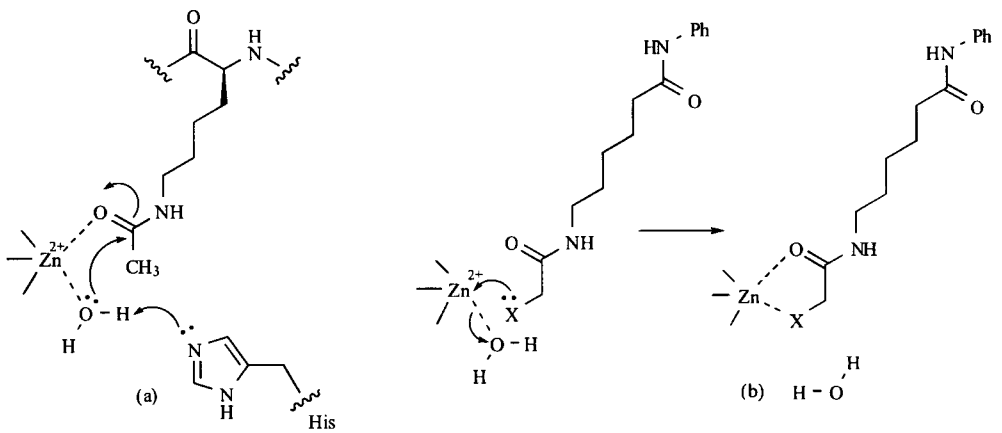

Fig. (17). Mechanism proposed for the deacetylation of acetylated lysine substrate (a), and model for the binding of hetero atom-containing substrate analogues to zinc ion (b).

31 and **32** did not possess inhibitory activity. Mercaptoacetamide **30** exhibited an IC_{50} of 0.39 μM and was found to be a competitive inhibitor versus acetylated

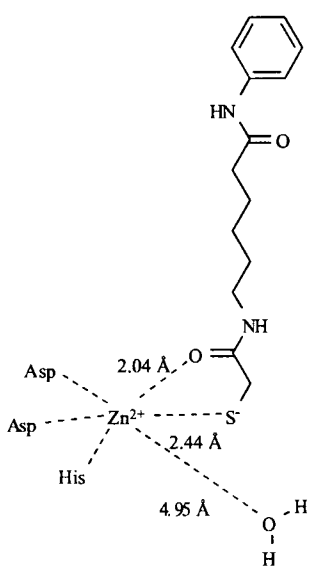

Fig. (18). Low energy conformation of **30** (IC_{50} = 0.39 μM) docked in the HDAC8 catalytic core.

Potent HDAC inhibitors with a mercaptoacetamide moiety have recently been reported independently by two research groups. Chen and co-workers have identified 8-quinolynyl compound **33** (IC_{50} = 0.044 μM) [72], and Anandan and co-workers have reported 3-quinolynyl compound **34** (IC_{50} = 1.1 μM) [73] (Fig. (**19**)). In addition, mercaptoethylamides such as **35** have also been reported to

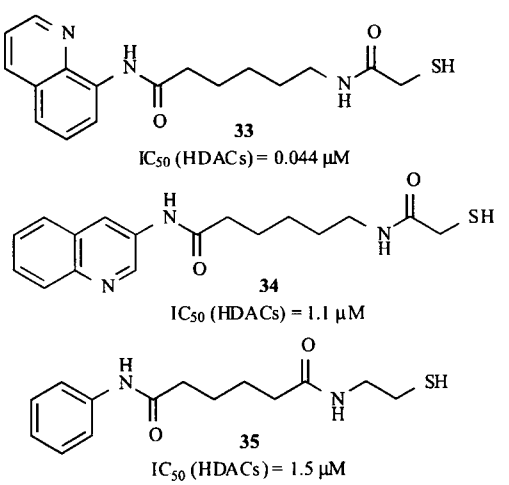

33
IC_{50} (HDACs) = 0.044 μM

34
IC_{50} (HDACs) = 1.1 μM

35
IC_{50} (HDACs) = 1.5 μM

Fig. (19). Mercaptoamide-based HDAC inhibitors.

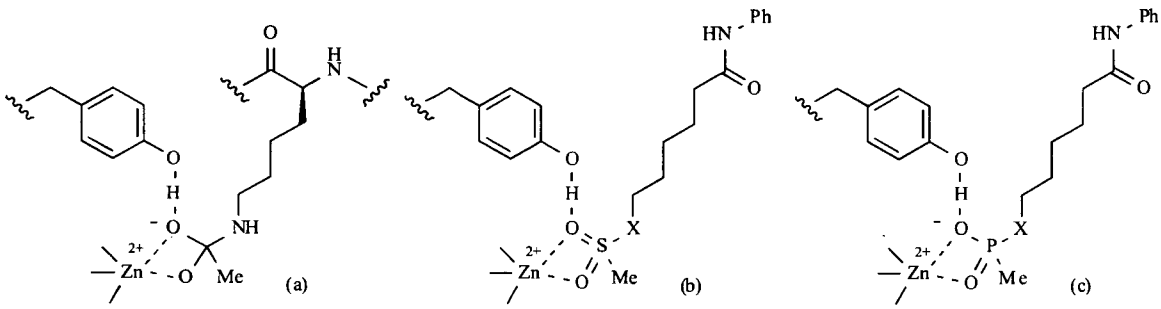

Fig. (20). Transition state proposed for HDACs (a), and models for the binding of sulfone derivatives (b) and phosphone derivatives (c).

inhibit HDACs with IC_{50}s of 1–100 μM [73]. Since mercaptoacetamides are reported as potent, long-lasting, and less toxic matrix metalloproteinase inhibitors [74, 75], they could be more improved HDAC inhibitors.

Sulfones and Phosphones as Transition State Analogues

Transition state (TS) analogue inhibitors have been reported independently by us [71] and Etzkorn et al [76]. The TS of HDAC deacetylation was estimated to include a tetrahedral carbon [18-20] (Fig. (**20**)a) as with other zinc proteases [77]. Sulfone and phosphone derivatives could be TS analogue inhibitors because they have strong similarity with the TS of amide bond hydrolysis (Fig. (**20**)b,c). Among these TS analogues, sulfone **36** [71] and phosphonamidate **37** [76] (Fig. (**21**)) inhibited HDACs at high micromolar concentrations. In addition, the antiproliferative activity of **37** against A2780 cancer cells (IC_{50} = 120 μM) was comparable to that of SAHA (IC_{50} = 150 μM).

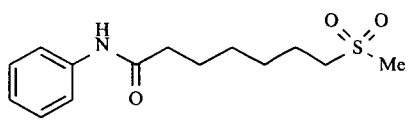

36
IC_{50} (HDACs) = 230 μM

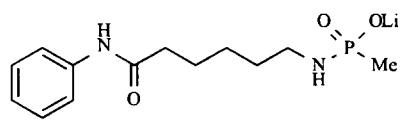

37
IC_{50} (HDAC8) = 280 μM
IC_{50} (HDACs) = 570 μM
IC_{50} (HDLP) = 330 μM

Fig. (21). Transition state analogue HDAC inhibitors.

Miscellaneous

We recently presented SAHA-based non-hydroxamates **38–41** (Fig. (**22**)), as HDAC inhibitors, which were identified by structure-based drug design [68, 78, 79]. These compounds displayed anti-HDAC activities with IC_{50}s of 14–150 μM. Although their inhibitory activities are weaker than that of SAHA, sulfoxide **41** showed a certain type of selectivity (see the section Isozyme Selectivity).

Design and synthesis of 3-(4-aroyl-1*H*-2-pyrrolyl)-2-propene derivatives were reported by Mai et al [44]. Among them, barbiturate **42**, thiobarbiturate **43**, nitrile **44** and amidine **45** exhibited inhibitory activities against maize HDAC2 with IC_{50}s of 23–100 μM (Fig. (**23**)).

Some natural products have been reported to inhibit HDACs (Fig. (**24**)). Schreiber and co-workers reported that depudecin **46**, a metabolite isolated from the fungus Alternaria brassicicola, inhibits HDAC1 with an IC_{50} of 4.7 μM [80]. The mechanism of action of depudecin **46** is yet unclear, but it may inhibit HDACs irreversibly like trapoxin B **8**. Crews and co-workers isolated novel disulfide bromotyrosine derivatives such as psammaplins F **47** from the sponge *Pseudoceratina purpurea*, which were found to be highly potent HDAC inhibitors (IC_{50} of **47** = 2.1 nM) [81]. Interestingly, some of the psammaplins also showed inhibitory activity against semipurified DNA methyltransferase I. It is not known exactly how psammaplins inhibit these enzymes. Fusetani and co-workers isolated new cyclostellettamines such as dehydrocyclostellettamine D **48** from a marine sponge of the

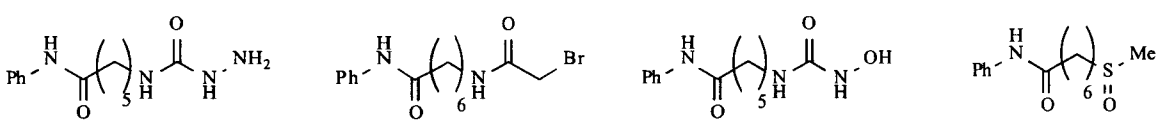

38
IC_{50}(HDACs) = 150 μM

39
IC_{50} (HDACs) = 14 μM

40
IC_{50} (HDACs) = 80 μM

41
IC_{50} (HDACs) = 48 μM

Fig. (22). SAHA-based non-hydroxamate HDAC inhibitors identified by structure-based drug design.

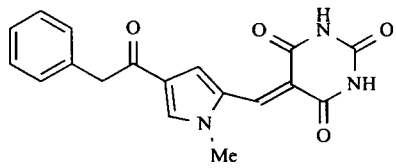

42
IC_{50} (maize HDAC2) = 100 μM

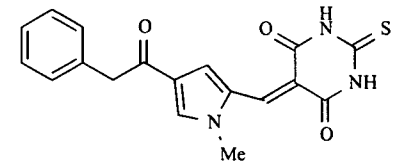

43
IC_{50} (maize HDAC2) = 85 μM

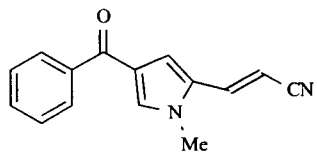

44
IC_{50} (maize HDAC2) = 27 μM

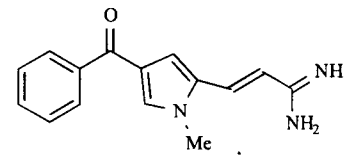

45
IC_{50} (maize HDAC2) = 23 μM

Fig. (23). 3-(4-Aroyl-1*H*-2-pyrrolyl)-2-propene derivatives.

genus *Xestospongia* [82]. These cyclostellettamines were found to inhibit HDACs derived from K562 human leukemia cells with IC_{50}s ranging from 17 to 80 μM. However, they showed cytotoxicity against P388, HeLa, and 3Y1 cells at lower concentrations (IC_{50} of 0.6–11 μM). These results indicate that these cyclostellettamines have biological activities other than inhibition of HDACs.

ISOZYME SELECTIVITY

The HDAC family is divided into two categories, zinc-dependent enzymes and NAD^+-dependent enzymes [1, 83]. The HDAC inhibitors described above are inhibitors of zinc-dependent enzymes. Thus far, eleven zinc-dependent HDAC family members have been identified and they are classified into two classes (Class I and Class II) based on sequence similarity (Table 1). Class I HDACs include HDAC1, HDAC2, HDAC3 and HDAC8, and show homology to the yeast protein RPD3. Class II HDACs include HDAC4, HDAC5, HDAC6, HDAC7, HDAC9 and HDAC10, and are homologous to the yeast enzyme HDA1. HDAC11, the most recently identified member, most likely belongs to Class I, although the sequence similarity is low [84]. Class I HDACs are expressed in the nuclei of most cell lines and are involved in the transcriptional repression of a number of genes [85-87]. On the contrary, the localization of Class II enzymes is not limited to the nucleus. They are also expressed in cytoplasm [88] and are associated with muscle differentiation block [89] and microtubule stability (see below). HDACs have been reported to be linked with carcinogenesis [90-92], while tissue-specifically expressed HDAC isozymes are known to play important roles in the generation and differentiation of normal tissues [89, 93-95].

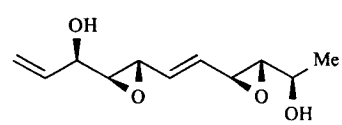

46: depudecin
IC_{50} (HDAC1) = 4.7 μM

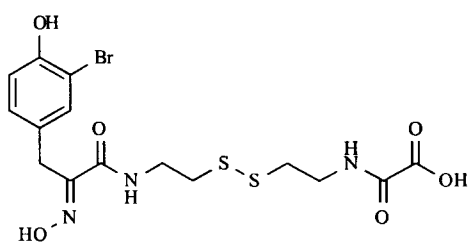

47: psammaplin F
IC_{50} (HDACs) = 2.1 nM

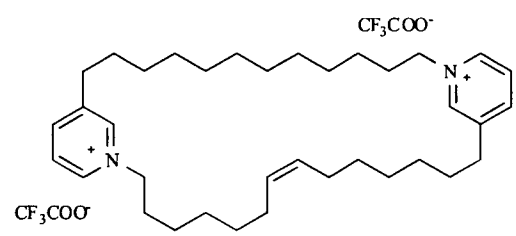

48: dehydrocyclostellettamine D
IC_{50} (HDACs) = 17 μM

Fig. (24). Structures of depudecin **46**, psammaplin F **47** and dehydrocyclostellettamine D **48**.

Table 1. Classification of Zinc-Dependent HDACs [1, 83-89]

HDAC	localization	function
Class I (RPD3 homologue)		
HDAC1	nucleus	transcription repression
HDAC2	nucleus	transcription repression
HDAC3	nucleus, cytoplasm	transcription repression
HDAC8	nucleus	transcription repression
HDAC11	nucleus	unknown
Class II (HDA1 homologue)		
HDAC4	nucleus, cytoplasm	transcription repression
		muscle differentiation block
HDAC5	nucleus, cytoplasm	transcription repression
		muscle differentiation block
HDAC6	cytoplasm	regulation of microtubule stability
		and function
HDAC7	nucleus, cytoplasm	transcription repression
		muscle differentiation block
HDAC9	nucleus, cytoplasm	unknown
HDAC10	cytoplasm	unknown

Therefore, isozyme-selective HDAC inhibitors are considered to be useful not only as tools for probing the biology of HDAC isozymes but as drugs with low toxicity. Interestingly, many non-hydroxamate HDAC inhibitors have shown isozyme selectivity. In this section, we describe the selectivity of non-hydroxamate HDAC inhibitors in enzyme assays and in cellular assays.

Table 2. Inhibitory activities of HDAC inhibitors against HDAC1 and HDAC6 [98]

Inhibitors	mean IC_{50} (nM)		HDAC6 IC_{50}/HDAC1 IC_{50}
	HDAC1	HDAC6	
TSA (**3**)	19	14	0.74
trapoxin B (**8**)	0.13	74	570
FK228 (**28**)	36	14,000	390
MS-275 (**10**)	250	>10,000,000	>40,000
sodium bytyrate (**4**)	170,000	>10,000,000	>59

Of the eleven HDAC isozymes, HDAC6 has been studied the most. HDAC6 is unique in that it is essentially cytoplasmic and has the interesting property of being capable of nucleocytoplasmic shuttling. In addition, HDAC6 is predominantly expressed in the testes, and is speculated to be involved in the differentiation of normal tissues [96]. It has been also reported that HDAC6 expression is correlated with breast cancer [97]. Thus, HDAC6-insensitive inhibitors could be medicines with less toxicity. Yoshida and co-workers investigated the in vitro inhibitory effects of a wide variety of HDAC inhibitors including non-hydroxamates on HDAC1 and HDAC6 [98]. As shown in Table 2, TSA **3**, a representative hydroxamate inhibitor, inhibited both HDAC1 and HDAC6. Although trapoxin B **8**, an inhibitor bearing epoxyketone, strongly inhibited HDAC1 at subnanomolar concentrations, it failed to inhibit HDAC6 at these concentrations. Like trapoxin B **8**, other non-hydroxamates such as sodium butyrate **4**, MS-275 **10** and FK228 **28** inhibited HDAC1 more than HDAC6.

HDAC6 has also been reported to be an α-tubulin deacetylase (TDAC) [99]. Unlike other HDAC isozymes, HDAC6 has two catalytic domains, one for histones (the HDAC site) and the other for α-tubulin (the TDAC site) [100, 101]. Inhibition of the TDAC site of HDAC6, which is responsible for the deacetylation of α-tubulin, is usually assessed by the accumulation of acetylated α-tubulin in a cellular assay (Western blot analysis) after treatment with inhibitor. Most hydroxamate HDAC inhibitors such as SAHA **1** and TSA **3** have been reported to cause both histone hyperacetylation and α-tubulin acetylation in cells, which suggests that these hydroxamates do not discriminate between TDAC (HDAC6) and the other isozymes [98, 99, 102, 103]. In contrast, the non-hydroxamate HDAC inhibitors that have been assessed for their effect on α-tubulin acetylation status do not cause an accumulation of acetylated α-tubulin and are presumably not inhibitors of the TDAC site of HDAC6 (Table 3). Schreiber and co-workers were the earliest to disclose non-hydroxamate HDAC inhibitors which are insensitive to the TDAC site of

Table 3. Effect on Acetylation of α-Tubulin

Inhibitors	Ac-α-tubulin[a]	References
Hydroxamic acids		
SAHA (1)	(+)	[103]
TSA (3)	(+)	[98, 99, 101, 102]
Non-hydroxamates		
histacin (14)	(-)	[28]
PAOA (15)	(-)	[56]
MS-275 (10)	(-)	[63]
sodium bytyrate (4)	(-)	[99]
trapoxin B (8)	(-)	[98, 99]
FK228 (28)	(-)	[102, 104]
α-ketoamide (19)	(-)	[63]
sulfoxide (41)	(-)	[79]

[a] (+) indicates an accumulation of acetylated α-tubulin while (-) indicates no effect on acetylation.

HDAC6. A multidimensional, high-throughput, cell-based screening of 7,392 small molecules prepared using a one-bead/one-stock solution strategy led to the identification of histacin **14**, which is inactive toward TDAC (HDAC6) in cells [28, 55]. These workers have also extended this finding by creating SAHA/*o*-aminoanilide hybrids such as PAOA **15** that inhibit nuclear HDAC isozymes over cytoplasmic TDAC (HDAC6) [56]. Another *o*-aminoanilde inhibitor MS-275 **10** was shown not to increase the acetylation state of α-tubulin, either [63]. It has been reported that the carboxylic acid sodium butyrate **4**, the epoxyketone trapoxin B **8** and the disulfide FK228 **28** show greater inhibition of nuclear HDACs than TDAC (HDAC6) in cells [98, 99, 102, 104]. Glaser and co-workers at Abbott found that α-ketoamide HDAC inhibitor **19** was selective for the TDAC site of HDAC6 in cells, although **19** did not distinguish between HDAC1/2 and HDAC6 in enzyme assays [63]. Very recently, we have reported that sulfoxide **41** showed great HDAC/TDAC selectivity in cellular assays [79].

It is surprising that non-hydroxamate HDAC inhibitors discriminated between HDAC6 and other isozymes in enzyme assays and cellular assays because the amino acid residues surrounding the zinc ion in the active site of HDACs are highly conserved [13, 55]. It is still unclear why non-hydroxamates distinguish well between HDAC6 and other isozymes. However, the nature of ZBG of HDAC inhibitors is an important factor determining the selectivity for HDAC6. As mentioned above, HDAC6 is estimated to be responsible for the differentiation of normal tissues such as the testis. Furthermore, the reversible acetylation of α-tubulin, which is partly regulated by HDAC6, is involved with microtubule stability [99]. Therefore, the isozyme selectivity of non-hydroxamates has important clinical implications for the development of new medicines without side effects caused by interference with nuclear homeostasis and microtubule dynamics associated with HDAC6.

PERSPECTIVE

Worldwide research on HDAC has led to the discovery of a number of structurally diverse inhibitors of HDACs. The first generation of HDAC inhibitors including SAHA, NVP-LAQ824 and MS-275 are currently in clinical trials. There is now strong evidence from clinical studies that these HDAC inhibitors are effective. The therapeutic potential is expected to increase when further positive clinical findings are unveiled. However, hydroxamic acid-based inhibitors have perceived liabilities such as poor pharmacokinetics, and the lack of isozyme selectivity of hydroxamates may cause severe toxicity. The discovery of non-hydroxamate HDAC inhibitors introduced in this review has provided the basis for the development of more improved HDAC inhibitors. Further study on non-hydroxamate HDAC inhibitors will also offer a basis on which to better design isozyme-selective inhibitors and to overcome the drawbacks of hydroxamates.

REFERENCES

[1] Hassig, C. A.; Schreiber, S. L. *Curr. Opin. Chem. Biol.* **1997**, *1*, 300.
[2] Kouzarides, T. *Curr. Opin. Genet. Dev.* **1999**, *9*, 40.
[3] Grozinger, C. M.; Schreiber, S. L. *Chem. Biol.* **2002**, *9*, 3.
[4] Taunton, J.; Hassig, C. A.; Schreiber, S. L. *Science* **1996**, *272*, 408.
[5] Sambucetti, L. C.; Fischer, D. D.; Zabludoff, S.; Kwon, P. O.; Chamberlin, H.; Trogani, N.; Xu, H.; Cohen, D. *J. Biol. Chem.* **1999**, *274*, 34940.
[6] Hirose, T.; Sowa, Y.; Takahashi, S.; Saito, S.; Yasuda, C.; Shindo, N.; Furuichi, K.; Sakai, T. *Oncogene* **2003**, *22*, 7762.
[7] Klisovic, D. D., Katz, S. E., Effron, D., Klisovic, M. I., Wickham, J., Parthun, M. R., Guimond, M., Marcucci, G. *Invest. Ophth. Vis. Sci.* **2003**, *44*, 2390.
[8] Leoni, F; Zaliani, A.; Bertolini, G.; Porro, G.; Pagani, P.; Pozzi, P.; Donà, G.; Fossati, G.; Sozzani, S.; Azam, T.; Bufler, P.; Fantuzzi, G.; Goncharov, I.; Kim, S. H.; Pomerantz, B. J.; Reznikov, L. L.; Siegmund, B.; Dinarello, C. A.; Mascagni, P. *Proc. Natl. Acad. Sci. U.S.A.* **2002**, *99*, 2995.
[9] Cao, H.; Stamatoyannopoulos, G.; Jung, M. *Blood* **2004**, *103*, 701.
[10] Jung, M. *Curr. Med. Chem.* **2001**, *8*, 1505.
[11] Arts, J.; de Schepper, S.; Van Emelen, K. *Curr. Med. Chem.* **2003**, *10*, 2342.
[12] Yoshida, M.; Matsuyama, A.; Komatsu, Y.; Nishino, N. *Curr. Med. Chem.* **2003**, *10*, 2351.
[13] Miller, T. A.; Witter, D. J.; Belvedere, S. *J. Med. Chem.* **2003**, *46*, 5097.
[14] Monneret, C. *Eur. J. Med. Chem.* **2005**, *40*, 1.
[15] Mai, A.; Massa, S.; Rotili, D.; Cerbara, I.; Valente, S.; Pezzi, R.; Simeoni, S.; Ragno, R. *Med. Res. Rev.* **2005**, *25*, 261.
[16] Richon, V. M.; Webb, Y.; Merger, R.; Sheppard, T.; Jursic, B.; Ngo, L.; Civoli, F.; Breslow, R.; Rifkind, R. A.; Marks, P. A. *Proc. Natl. Acad. Sci. U.S.A.* **1996**, *93*, 5705.
[17] Remiszewski, S. W. *Curr. Med. Chem.* **2003**, *10*, 2393.
[18] Finnin, M. S.; Donigian, J. R.; Cohen, A.; Richon, V. M.; Rifkind, R. A.; Marks, P. A.; Breslow, R.; Pavletich, N. P. *Nature* **1999**, *401*, 188.
[19] Somoza, J. R.; Skene, R. J.; Katz, B. A.; Mol, C.; Ho, J. D.; Jennings, A. J.; Luong, C.; Arvai, A.; Buggy, J. J.; Chi, E.; Tang, J.; Sang, B.-C.; Verner, E.; Wynands, R.; Leahy, E. M.; Dougan, D. R.; Snell, G.; Navre, M.; Knuth, M. W.; Swanson, R. V.; McRee, D. E.; Tari, L. W. *Structure* **2004**, *12*, 1325.
[20] Vannini, A.; Volpari, C.; Filocamo, G.; Casavola, E. C.; Brunetti, M.; Renzoni, D.; Chakravarty, P.; Paolini, C.; Francesco, R. D.; Gallinari, P.; Steinkühler, C.; Marco, S. D. *Proc. Natl. Acad. Sci. U.S.A.*, **2004**, *101*, 15064.
[21] Yoshida, M.; Horinouchi, S.; Beppu, T. *BioEssays* **1995**, *17*, 423.
[22] Vanhaecke, T.; Papeleu, P.; Elaut, G.; Rogiers, V. *Curr. Med. Chem.* **2004**, *11*, 1629.

[23] Mulder, G. J.; Meerman, J. H. *Environ. Health Perspect.* **1983**, *49*, 27.

[24] Vassiliou, S.; Mucha, A.; Cuniasse, P.; Georgiadis, D.; Lucet-Levannier, K.; Beau, F.; Kannan, R.; Murphy, G.; Knaeuper, V.; Rio, M. C.; Basset, P.; Yiotakis, A.; Dive, V. *J. Med. Chem.* **1999**, *42*, 2610.

[25] Kelly, W. K.; Richon, V. M.; O'Connor, O.; Curley, T.; MacGregor-Curtelli, B.; Tong, W.; Klang, M.; Schwartz, L.; Richardson, S.; Rosa, E.; Drobnjak, M.; Cordon-Cordo, C.; Chiao, J. H.; Rifkind, R.; Marks, P. A.; Scher, H. *Clin. Cancer Res.* **2003**, *9*, 3578.

[26] Qiu, L.; Kelso, M. J.; Hansen, C.; West, M. L.; Fairlie, D. P.; Parsons, P. G. *Br. J. Cancer* **1999**, *80*, 1252.

[27] Whittaker, M.; Floyd, C. D.; Brown, P.; Gearing, A. *J. Chem. Rev.* **1999**, *99*, 2735.

[28] Haggarty, S. J.; Koeller, K. M.; Wong, J. C.; Butcher, R. A.; Schreiber, S. L. *Chem. Biol.* **2003**, *10*, 383.

[29] Mai, A.; Massa, S.; Pezzi, R.; Simeoni, S.; Rotili, D.; Nebbioso, A.; Scognamiglio, A.; Altucci, L.; Loidl, P.; Brosch, G. *J. Med. Chem.* **2005**, *48*, 3344.

[30] Watson, J.; Glasg, M. B. *Lancet* **1933**, 746.

[31] Chen, J. S.; Faller, D. V. *Curr. Cancer Drug Targets* **2003**, *3*, 219.

[32] Gottlicher, M.; Minucci, S.; Zhu, P.; Kramer, O. H.; Schimpf, A.; Giavara, S.; Sleeman, J. P.; Lo Coco, F.; Nervi, C.; Pelicci, P. G.; Heinzel, T. *EMBO J.* **2001**, *20*, 6969.

[33] Phiel, C. J.; Zhang, F.; Huang, E. Y.; Guenther, M. G.; Lazar, M. A.; Klein, P. S. *J. Biol. Chem.* **2001**, *276*, 36734.

[34] Lea, M. A.; Sura, M.; desBordes, C. *Cancer Chemo. Pharm.* **2004**, *54*, 57.

[35] Warrell, R. P.; He, L.; Richon, V.; Calleja, E.; Pandolfi, P. P. *J. Natl. Cancer Inst.* **1998**, *90*, 1621.

[36] McLaughlin, F.; La Thangue, N. B. *Biochem. Pharmacol.* **2004**, *68*, 1139.

[37] Gross, M. L.; McCrery, D.; Crow, F.; Tomer, K. B.; Pope, M. R.; Ciuffetti, L. M.; Knoche, H. W.; Daly, J. M.; Dunkle, L. D. *Tetrahedron Lett.* **1982**, *23*, 5381.

[38] Liesch, J. M.; Sweeley, C. C.; Staffeld, G. D.; Anderson, M. S.; Weber, D. J.; Scheffer, R. P. *Tetrahedron* **1982**, *38*, 45.

[39] Kim, S. -D.; Knoche, H. W.; Dunkle, L. D.; McCrery, D. A.; Tomer, K. B. *Tetrahedron Lett.* **1985**, *26*, 969.

[40] Tanis, S. P.; Horenstein, B. A.; Scheffer, R. P.; Rasmussen, J. B. *Heterocycles* **1986**, *24*, 3423.

[41] Itazaki, H.; Nagashima, K.; Sugita, K.; Yoshida, H.; Kawamura, Y.; Yasuda, Y.; Matsumoto, K.; Ishii, K.; Uotani, N.; Nakai, H.; Terui, A.; Yoshimatsu, S.; Ikenishi, Y.; Nakagawa, Y. *J. Antibiot.* **1990**, *63*, 1524.

[42] Kijima, M.; Yoshida, M.; Sugita, K.; Horinouchi, S.; Beppu, T. *J. Biol. Chem.* **1993**, *268*, 22429.

[43] Brosch, G.; Ransom, R.; Lechner, T.; Walton, J. D.; Loidl, P. *Plant Cell* **1995**, *7*, 1941.

[44] Mai, A.; Massa, S.; Rango, R.; Cerbara, I.; Jesacher, F.; Loidl, P.; Brosch, G. *J. Med. Chem.* **2003**, *46*, 512.

[45] Darkin-Rattray, S. J.; Gurnett, A. M.; Myers, R. W.; Dulski, P. M.; Crumley, T. M.; Allocco, J. J.; Cannova, C.; Meinke, P. T.; Colletti, S. L.; Bednarek, M. A.; Singh, S. B.; Goetz, M. A.; Dombrowski, A. W.; Polishook, J. D.; Schmatz, D. M. *Proc. Natl. Acad. Sci. U.S.A.* **1996**, *93*, 13143.

[46] Singh, S. B.; Zink, D. L.; Liesch, J. M.; Dombrowski, A. W.; Darkin-Rattray, S. J.; Schmatz, D. M.; Goetz, M. A. *Org. Lett.* **2001**, *3*, 2815.

[47] Singh, S. B.; Zink, D. L.; Liesch, J. M.; Mosley, R. T.; Dombrowski, A. W.; Bills, G. F.; Darkin-Rattray, S. J.; Schmatz, D. M.; Goetz, M. A. *J. Org. Chem.* **2002**, *67*, 815.

[48] Suzuki, T.; Ando, T.; Tsuchiya, K.; Fukazawa, N.; Saito, A.; Mariko, Y.; Yamashita, T.; Nakanishi, O. *J. Med. Chem.* **1999**, *42*, 3001.

[49] Saito, A.; Yamashita, T.; Mariko, Y.; Nosaka, Y.; Tsuchiya, K.; Ando, T.; Suzuki, T.; Tsuruno, T.; Nakanishi, O. *Proc. Natl. Acad. Sci. U.S.A.* **1999**, *96*, 4592.

[50] Kraker, A. J.; Mizzen, C. A.; Hartl, B. G.; Miin, J.; Allis, C. D.; Merriman, R. L. *Mol. Cancer Ther.* **2003**, *2*, 401.

[51] Bouchain, G.; Leit, S.; Frechette, S.; Khalil, E. A.; Lavoie, R.; Moradei, O.; Woo, S. H.; Fournel, M.; Yan, P. T.; Kalita, A.; Trachy-Bourget, M. -C.; Beaulieu, C.; Li, Z.; Robert, M. -F.; MacLeod, A. R.; Besterman, J. M.; Delorme, D. *J. Med. Chem.* **2003**, *46*, 820.

[52] Fournel, M.; Trachy-Bourget, M. -C.; Theresa Yan, P.; Kalita, A.; Bonfils, C.; Beaulieu, C.; Frechette, S.; Leit, S.; Abou-Khalil, E.; Woo, S. -H.; Delorme, D.; MacLeod, A. R.; Besterman, J. M.; Li, Z. *Cancer Res.* **2002**, *62*, 4325.

[53] Vaisburg, A.; Bernstein, N.; Frechette, S.; Allan, M.; Abou-Khalil, E.; Leit, S.; Moradei, O.; Bouchain, G.; Wang, J.; Woo, S. H.; Fournel, M.; Yan, P. T.; Trachy-Bourget, M. -C.; Kalita, A.; Beaulieu, C.; Li, Z.; MacLeod, A. R.; Besterman, J. M.; Delorme, D. *Bioorg. Med. Chem. Lett.* **2004**, *14*, 283.

[54] Bouchain, G.; Delorme, D. *Curr. Med. Chem.* **2003**, *10*, 2359.

[55] Sternson, S. M.; Wong, J. C.; Grozinger, C. M.; Schreiber, S. L. *Org. Lett.* **2001**, *3*, 4239.

[56] Wong, J. C.; Hong, R.; Schreiber, S. L. *J. Am. Chem. Soc.* **2003**, *125*, 5586.

[57] Woo, S. H.; Frechette, S.; Khalil, E. A.; Bouchain, G.; Vaisburg, A.; Bernstein, N.; Moradei, O.; Leit, S.; Allan, M.; Fournel, M.; Trachy-Bourget, M. -C.; Li, Z.; Besterman, J. M.; Delorme, D. *J. Med. Chem.* **2002**, *45*, 2877.

[58] Curtin, M.; Glaser, K. *Curr. Med. Chem.* **2003**, *10*, 2373.

[59] Frey, R. R.; Wada, C. K.; Garland, R. B.; Curtin, M. L.; Michaelides, M. R.; Li, J.; Pease, L. J.; Glaser, K. B.; Marcotte, P. A.; Bouska, J. J.; Murphy, S. S.; Davidsen, S. K. *Bioorg. Med. Chem. Lett.* **2002**, *12*, 3443.

[60] Jose, B.; Oniki, Y.; Kato, T.; Nishino, N.; Sumida Y.; Yoshida, M. *Bioorg. Med. Chem. Lett.* **2004**, *14*, 5343.

[61] Wada, C. K.; Frey, R. R.; Ji, Z.; Curtin, M. L.; Garland, R. B.; Holms, J. H.; Li, J.; Pease, L. J.; Guo, J.; Glaser, K. B.; Marcotte, P. A.; Richardson, P. L.; Murphy, S. S.; Bouska, J. J.; Tapang, P.; Magoc, T. J.; Albert, D. H.; Davidsen, S. K.; Michaelides, M. R. *Bioorg. Med. Chem. Lett.* **2003**, *13*, 3331.

[62] Vasudevan, A.; Ji, Z.; Frey, R. R.; Wada, C. K.; Steinman, D.; Heyman, H. R.; Guo, Y.; Curtin, M. L.; Guo, J.; Li, J.; Pease, L.; Glaser, K. B.; Marcotte, P. A.; Bouska, J. J.; Davidsen, S. K.; Michaelides, M. R. *Bioorg. Med. Chem. Lett.* **2003**, *13*, 3909.

[63] Glaser, K. B.; Li, J.; Pease, L. J.; Staver, M. J.; Marcotte, P. A.; Guo, J.; Frey, R. R.; Garland, R. B.; Heyman, H. R.; Wada, C. K.; Vasudevan, A.; Michaelides, M. R.; Davidsen, S. K.; Curtin, M. L. *Biochem. Biophys. Res. Commun.* **2004**, *325*, 683.

[64] Wu, T. Y. H.; Hassig, C.; Wu, Y.; Ding, S.; Schultz, P. G. *Bioorg. Med. Chem. Lett.* **2004**, *14*, 449.

[65] Nishino, N.; Yoshikawa, D.; Watanabe, L. A.; Kato, T.; Jose, B.; Komatsu, Y.; Sumida, Y.; Yoshida, M. *Bioorg. Med. Chem. Lett.* **2004**, *14*, 2427.

[66] Ondetti, M. A.; Rubin, B.; Cushman, D. W. *Science* **1977**, *196*, 441.

[67] Suzuki, T.; Kouketsu, A.; Matsuura, A.; Kohara, A.; Ninomiya, S.; Kohda, K.; Miyata, N. *Bioorg. Med. Chem. Lett.* **2004**, *14*, 3313.

[68] Suzuki, T.; Nagano, Y.; Kouketsu, A.; Matsuura, A.; Maruyama, S.; Kurotaki, M.; Nakagawa, H.; Miyata, N. *J. Med. Chem.* **2005**, *48*, 1019.

[69] Furumai, R.; Matsuyama, A.; Kobashi, N.; Lee, K. -H.; Nishiyama, M.; Nakajima, H.; Tanaka, A.; Komatsu, Y.; Nishino, N.; Yoshida, M.; Horinouchi, S. *Cancer Res.* **2002**, *62*, 4916.

[70] Nishino, N.; Jose, B.; Okamura, S.; Ebisusaki, S.; Kato, T.; Sumida, Y.; Yoshida, M. *Org. Lett.* **2003**, *5*, 5079.

[71] Suzuki, T.; Matsuura, A.; Kouketsu, A.; Nakagawa, H.; Miyata, N. *Bioorg. Med. Chem. Lett.* **2005**, *15*, 331.

[72] Chen, B.; Petukhov, P. A.; Jung, M.; Velena, A.; Elisceva, E.; Dritschilo, A.; Kozikowski, A. P. *Bioorg. Med. Chem. Lett.* **2005**, *15*, 1389.

[73] Anandan, S. -K.; Ward, J. S.; Brokx, R. D.; Bray, M. R.; Patel, D. V.; Xiao, X. -X. *Bioorg. Med. Chem. Lett.* **2005**, *15*, 1969.

[74] Rizvi, N. A.; Humphrey, J. S.; Ness, E. A.; Johnson, M. D.; Gupta, E.; Williams, K.; Daly, D. J.; Sonnichsen, D.; Conway, D.; Marshall, J.; Hurwitz, H. *Clin. Cancer Res.* **2004**, *10*, 1963.

[75] Baxter, A. D.; Bird, J.; Bhogal, R.; Massil, T.; Minton, K. J.; Montana, J.; Owen, D. A. *Bioog. Med. Chem. Lett.* **1997**, *7*, 897.

[76] Kapustin, G. V.; Féjer, G.; Gronlund, J. L.; McCafferty, D. G.; Seto, E.; Etzkorn, F. A. *Org. Lett.* **2003**, *5*, 3053.

[77] Christianson, D. W.; Lipscomb, W. N. *Acc. Chem. Res.* **1989**, *22*, 62.

[78] Suzuki, T.; Nagano, Y.; Matsuura, A.; Kohara, A.; Ninomiya, S.; Kohda, K.; Miyata, N. *Bioorg. Med. Chem. Lett.* **2003**, *13*, 4321.

[79] Suzuki, T.; Matsuura, A.; Kouketsu, A.; Hisakawa, S.; Nakagawa, H.; Miyata, N. *Bioorg. Med. Chem.* **2005**, *13*, 4332.

[80] Kwon, H. J.; Owa, T.; Hassig, C. A.; Shimada, J.; Schreiber, S. L. *Proc. Natl. Acad. Sci. U.S.A.* **1998**, *95*, 3356.

[81] Piña, I. C.; Gautschi, J. T.; Wang, G. -Y. -S.; Sanders, M. L.; Schmitz, F. J.; France, D.; Cornell-Kennon, S.; Sambucetti, L. C.; Remiszewski, S. W.; Perez, L. B.; Bair, K. W.; Crews, P. *J. Org. Chem.* **2003**, *68*, 3866.
[82] Oku, N.; Nagai, K.; Shindoh, N.; Terada, Y.; van Soest, R. W. M.; Matsunaga, S.; Fusetani, N. *Bioog. Med. Chem. Lett.* **2004**, *14*, 2617.
[83] Khochbin, S.; Verdel, A.; Lemercier, C.; Seigneurin-Berny, D. *Curr. Opin. Genet. Dev.* **2001**, *11*, 162.
[84] Gao, L.; Cueto, M. A.; Asselbergs, F.; Atadja, P. *J. Biol. Chem.* **2002**, *277*, 25748.
[85] Robertson, K. D.; Wolffe, A. P. *Nature Rev. Genet.* **2000**, *1*, 11.
[86] Feng, Q.; Zhang, Y. *Genes & Dev.* **2001**, *15*, 827.
[87] Fuks, F.; Burgers, W. A.; Godin, N.; Kasai, M.; Kouzarides, T. *EMBO J.* **2001**, *20*, 2536.
[88] Verdin, E.; Dequiedt, F.; Kasler, H. G. *Trends Genet.* **2003**, *19*, 286.
[89] Mckinsey, T. A.; Zhang, C. L.; Lu, J.; Olson, E. N. *Nature* **2000**, *408*, 106.
[90] Lin, R. L.; Nagy, L.; Inoue, S.; Shao, W.; Miller, W. J.; Evans, R. M. *Nature* **1998**, *391*, 811.
[91] Grignani, F.; De Matteis, S.; Nervi, C.; Tomassoni, L.; Gelmetti, V.; Cioce, M.; Fanelli, M.; Ruthardt, M.; Ferrara, F. F.; Zamir, I.; Seiser, C.; Grignani, F.; Lazar, M. A.; Minucci, S.; Pelicci, P. G. *Nature* **1998**, *391*, 815.
[92] Juan, L. -J.; Shia, W. -J.; Chen, M. -H.; Yang, W. -M.; Seto, E.; Lin, Y. -S.; Wu, C. -W. *J. Biol. Chem.* **2000**, *275*, 20436.
[93] Verdel, A.; Khochbin, S. *J. Biol. Chem.* **1999**, *274*, 2440.
[94] Zhang, C. L.; McKinsey, T. A.; Chang, S.; Antos, C. L.; Hill, J. A.; Olson, E. N. *Cell* **2002**, *110*, 479.
[95] Dequiedt, F.; Kasler, H.; Fischle, W.; Kiermer, V.; Weinstein, M.; Herndier, B. G.; Verdin, E. *Immunity* **2003**, *18*, 687.
[96] Seigneurin-Berny, D.; Verdel, A.; Curtet, S.; Lemercier, C.; Garin, J.; Rousseaux, S.; Khochbin, S. *Mol. Cell. Biol.* **2001**, *21*, 8035.
[97] Zhang, Z.; Yamashita, H.; Toyama, T.; Sugiura, H.; Omoto, Y.; Ando, Y.; Mita, K.; Hamaguchi, M.; Hayashi, S.; Iwase, H. *Clin. Cancer Res.* **2004**, *10*, 6962.
[98] Matsuyama, A.; Yoshimatsu, Y.; Shimazu,T.; Sumida, Y.; Osada, H.; Komatsu, Y.; Nishino, N.; Khochbin, S.; Horinouchi, S.; Yoshida, M. *EMBO J.* **2002**, *21*, 6820.
[99] Hubbert, C.; Guardiola, A.; Shao, R.; Kawaguchi, Y.; Ito, A.; Nixon, A.; Yoshida, M.; Wang, X.; Yao, T. *Nature* **2002**, *417*, 455.
[100] Grozinger, C. M.; Hassig, C. A.; Schreiber, S. L. *Proc. Natl. Acad. Sci. U.S.A.* **1999**, *96*, 4868.
[101] Haggarty, S. J.; Koeller, K. M.; Wong, J. C.; Grozinger, C. M.; Schreiber, S. L. *Proc. Natl. Acad. Sci. U.S.A.* **2003**, *100*, 4389.
[102] Blagosklonny, M. V., Robey, R.; Sackett, D. L.; Du, L.; Traganos, F.; Darzynkiewicz, Z.; Fojo, T.; Bates, S. E. *Mol. Cancer. Ther.* **2002**, *1*. 937.
[103] Koeller, K. M.; Haggarty, S. J.; Perkins, B. D.; Leykin, I.; Wong, J. C.; Kao, M. J.; Schreiber, S. L. *Chem. Biol.* **2003**, *10*, 397.
[104] Warrener, R.; Beamish, H.; Burgess, A.; Waterhouse, N. J.; Giles, N.; Fairlie, D.; Gabrielli, B. *FASEB J.* **2003**, *17*, 1550.

Available online at www.sciencedirect.com
SCIENCE DIRECT®
Mutation Research 586 (2005) 1–17
Genetic Toxicology and Environmental Mutagenesis
www.elsevier.com/locate/gentox
Community address: www.elsevier.com/locate/mutres

Nitrogen-substitution effect on in vivo mutagenicity of chrysene

Katsuya Yamada [a], Takayoshi Suzuki [b,c], Arihiro Kohara [b], Taka-aki Kato [a], Makoto Hayashi [b], Takaharu Mizutani [a], Ken-ichi Saeki [a,*]

[a] *Graduate School of Pharmaceutical Sciences, Nagoya City University, Tanabedori, Mizuho-ku, Nagoya 467-8603, Japan*
[b] *Division of Genetics and Mutagenesis, National Institute of Health Sciences, 1-18-1 Kamiyoga, Setagaya-ku, Tokyo 158-8501, Japan*
[c] *Division of Cellular and Gene Therapy Products, National Institute of Health Sciences, 1-18-1 Kamiyoga, Setagaya-ku, Tokyo 158-8501, Japan*

Received 11 March 2005; received in revised form 28 April 2005; accepted 6 May 2005

Abstract

We have previously reported the in vivo mutagenicity of aza-polycyclic aromatic hydrocarbons (azaPAHs), such as quinoline, benzo[*f*]quinoline, benzo[*h*]quinoline, 1,7-phenanthroline and 10-azabenzo[*a*]pyrene. The 1,10-diazachrysene (1,10-DAC) and 4,10-DAC, nitrogen-substituted analogs of chrysene, were shown to exhibit mutagenicity in *Salmonella typhimurium* TA100 in the presence of rat liver S9 and human liver microsomes in our previous report, although DACs could not be converted to a bay-region diol epoxide, the ultimate active form of chrysene, because of their nitrogen atoms. In the present study, we tested in vivo mutagenicity of DACs compared with chrysene using the *lacZ* transgenic mouse (Muta™Mouse) to evaluate the effect of the nitrogen substitution. DACs- and chrysene-induced mutation in all of the six organs examined (liver, spleen, lung, kidney, bone marrow and colon). The mutant frequencies obtained with chrysene showed only small differences between the organs examined and ranged from 1.5 to 3 times the spontaneous frequency. The 4,10-DAC was more mutagenic than chrysene in all the organs tested. The highest *lacZ* mutation frequency was observed in the lung of 4,10-DAC-treated mice and it was 19 and 6 times the spontaneous frequency and the frequency induced by chrysene, respectively. The 1,10-DAC induced *lacZ* mutation in the lung with a frequency 4.3- and 1.5-fold higher than in the control and chrysene-treated mice, respectively, although the mutant frequencies in the other organs of 1,10-DAC-treated mice were almost equivalent to those of chrysene-treated mice. Not only chrysene but also DACs depressed the G:C to A:T transition and increased the G:C to T:A transversion in the liver and lung. These results suggest that the two types of nitrogen substitutions in the chrysene structure may enhance mutagenicity in the mouse lung, although they showed no difference in the target-organ specificity and the mutation spectrum.

Keywords: Aza-substitution; In vivo mutagenesis assay; Mutation spectrum

1. Introduction

We have been investigating the mutagenicity of aza-polycyclic aromatic hydrocarbons (azaPAHs) with

* Corresponding author. Tel.: +81 52 836 3485; fax: +81 52 834 9309.
E-mail address: saeki@phar.nagoya-cu.ac.jp (K. Saeki).

1383-5718/$ – see front matter © 2005 Elsevier B.V. All rights reserved.
doi:10.1016/j.mrgentox.2005.05.012

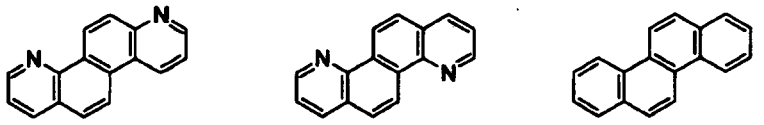

Fig. 1. Chemical structures of 1,10-DAC, 4,10-DAC and chrysene.

special attention to their metabolic activation mechanism. The 10-azabenzo[*a*]pyrene (10-azaBaP), a 10-aza-analog of benzo[*a*]pyrene (BaP), was reported to be as mutagenic as BaP in *Salmonella typhymurium* TA100 in the presence of PCB-treated rat liver S9 [1,2], although 10-azaBaP could not be converted to a bay-region diol epoxide, the ultimate mutagenic form of BaP [3,4], because of its nitrogen atom. We have previously reported that 10-azaBaP showed a higher mutagenicity than BaP in the Ames test using pooled human liver S9 [5]. However, in the in vivo mutagenesis assay system using the *lacZ* transgenic mouse (Muta™Mouse), 10-azaBaP was mutagenic only in the liver and colon and showed much less mutagenicity than BaP, which showed high mutagenicity in all of the organs tested [5]. Thus, 10-azaBaP interestingly showed differences in mutagenicity between the in vitro and in vivo assay systems.

We have also reported that quinoline, an aza-analog of naphthalene, one of simplest azaPAHs and a hepatocarcinogen [6,7], showed mutagenicity only in the liver of Muta™Mouse [8]. We also observed that it caused remarkable induction of G:C to C:G transversion [9] and suggested that it might be metabolically activated in the pyridine moiety to the ultimate mutagenic form [10]. Its active form was supposed to be an enamine epoxide (1,4-hydrated 2,3-epoxide), which would be responsible for the mutagenic modification of DNA [11–14]. Furthermore, three trycyclic azaPAHs, i.e., benzo[*f*]quinoline, benzo[*h*]quinoline and 1,7-phenanthroline, were shown to exhibit mutagenicity in Muta™Mouse in our previous report [15]. Benzo[*h*]quinoline and 1,7-phenanthroline were suggested to be converted to the ultimate genotoxic form in the pyridine moiety [16].

1,10-Diazachrysene (1,10-DAC) and 4,10-DAC are diaza-analogs of chrysene (Fig. 1), consisting of two quinoline moieties, and have structures similar to 10-azaBaP. We have previously reported that these DACs showed mutagenicity in Ames tests in the presence of rat liver S9 or human liver microsomes [17], although formation of the bay-region diol epoxide from DACs seemed impossible because of their nitrogen atoms. DACs have not been found in our living environments, but these are expected to be useful compounds to investigate the nature of mutagenicity in azaPAHs.

In the present study, we undertook to investigate the in vivo mutagenicity of DACs in comparison with chrysene by the in vivo mutation assay system using the *lacZ* transgenic mouse (Muta™Mouse) to evaluate the nitrogen-substitution effect in the chrysene skeleton on their mutagenicity.

2. Materials and methods

2.1. Materials

Chrysene (CAS Registry No. 218-01-9) and phenyl-β-D-galactoside (P-gal) were purchased from Sigma Chemical Co. (St. Louis, MO), proteinase K and olive oil from Wako Pure Chemicals (Osaka) and RNase from Boehringer Mannheim. The 1,10-DAC (CAS Registry No. 218-21-3) and 4,10-DAC (CAS Registry No. 218-34-8) were synthesized in this laboratory according to the reported methods [18].

2.2. In vivo mutagenesis assays using Muta™Mouse

2.2.1. Animals and treatments

Male Muta™Mice, at 7–8 weeks of age, were supplied by COVANCE Research Products (PA, USA) and acclimatized for 1 week before use. Chrysene and 4,10-DAC dissolved in olive oil (10 mL/kg body weight)

were injected intraperitoneally into four mice each at a single dose of 200 mg/kg once a week for 4 consecutive weeks (800 mg/kg in total). The 1,10-DAC dissolved in olive oil (10 mL/kg body weight) was injected into four mice at a single dose of 100 mg/kg similarly (400 mg/kg in total). Four control mice were given 10 mL olive oil/kg.

2.2.2. Tissues and DNA isolation

All mice were killed by cervical dislocation 7 days after the last administration of test chemicals. The liver, spleen, lung, kidney, bone marrow and colon were immediately extirpated, frozen in liquid nitrogen and stored at −80 °C until DNA extraction. The genomic DNA was extracted from each tissue by the phenol/chloroform method according to the Muta™Mouse/PS Mutation Assay Manual (Corning Hazleton, 1995). The isolated DNA, which was precipitated with ethanol, was air-dried and dissolved in an appropriate volume (20–200 μL) of TE-4 buffer (10 mM Tris–HCl at pH 8.0 containing 4 mM EDTA) at room temperature overnight. The DNA solution thus prepared was stored at 4 °C.

2.2.3. In vitro packaging

The lambda gt10/*lacZ* vector could be efficiently recovered by in vitro packaging reactions [19]. Our homemade packaging extract (HM) consisting of sonic extract (SE) of *Escherichia coli* NM759 and freeze–thaw lysate (FTL) of *E. coli* BHB2688 was prepared according to the method of Gunther et al. [20]. As a general procedure for handling the HM extract, approximately, 5 μg DNA was mixed with 15 μL of FTL and 30 μL of SE and incubated at 37 °C for 90 min. Then SE and FTL were added again and the mixture was incubated for another 90 min. The reaction was terminated by the addition of an appropriate volume of SM buffer (50 mM Tris–HCl at pH 7.5, 10 mM $MgSO_4$, 100 mM NaCl and 0.01% gelatin) and the mixture was stored at 4 °C. By this procedure, the lambda gt10 vector to form an infectious phage was efficiently rescued from genomic DNA.

2.2.4. Mutation assays

2.2.4.1. lacZ mutant frequency determination. The positive selection for *lacZ* mutants was performed as previously reported [21–23]. Briefly, the phage

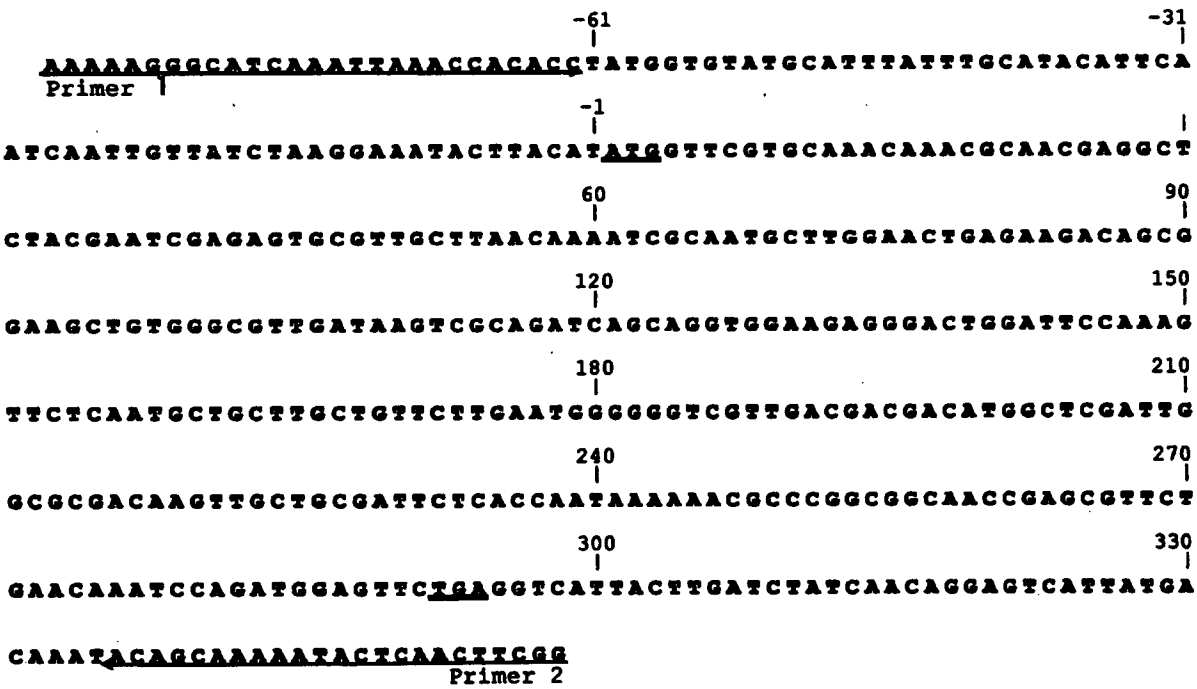

Fig. 2. Sequence map of the *cII* gene; primers used for PCR amplification and sequencing are shown by arrows. The PCR gives 446 bp products that involve the entire (294 bp) *cII* gene. Initiation and stop codons are underlined.

Table 1
Mutant frequencies induced by 1,10-DAC, 4,10-DAC and chrysene in six organs of Muta™Mouse

Tissue	Treatment	*lacZ* assay				*cII* assay			
		Individual animal data			Average ± S.D.	Individual animal data			Average ±S.D.
		No. of phages analyzed	No. of mutants	MF × 10^6	MF × 10^6	No. of phages analyzed	No. of mutants	MF × 10^6	MF × 10^6
Liver	Control (olive oil)	463000	36	77.8		1547000	31	20.0	
		173000	12	69.4		602000	20	33.2	
		1899000	247	130.1		1618000	47	29.0	
		396000	30	75.8	88.2 ± 24.3	1398000	22	15.7	24.5 ± 7.0
	1,10-DAC	391000	77	196.9		1299000	90	69.3	
		1126000	127	112.8		989000	40	40.4	
		371500	63	169.6		1805000	72	39.9	
		244000	36	147.5	156.7 ± 30.8*	1095000	23	21.0	42.7 ± 17.3
	4,10-DAC	192000	72	375.0		731000	79	108.1	
		355500	193	542.9		1446000	182	125.9	
		506500	225	444.2		2080000	233	112.0	
		503000	308	612.3	493.6 ± 90.9**	1751000	311	177.6	130.9 ± 27.8**
	Chrysene	452500	98	216.6		1025000	51	49.8	
		322500	88	272.9		1220000	81	66.4	
		362500	88	242.8		1343000	68	50.6	
		522000	89	170.5	225.7 ± 37.6**	1799000	60	33.4	50.0 ± 11.7*
Spleen	Control (olive oil)	866000	47	54.3		966000	14	14.5	
		1145000	59	51.5		1180000	25	21.2	
		870000	36	41.4		1024000	34	33.2	
		653500	23	35.2	45.6 ± 7.7	1039000	15	14.4	20.8 ± 7.7
	1,10-DAC	1700500	150	88.2		1550000	70	45.2	
		769000	77	100.1		909000	59	64.9	
		1252000	125	99.8		2119000	129	60.9	
		1316000	131	99.5	96.9 ± 5.0**	1837000	110	59.9	57.7 ± 7.5**
	4,10-DAC	469500	109	232.2		550000	56	101.8	
		1506000	525	348.6		1754000	260	148.2	
		1410000	374	265.2		2071000	268	129.4	
		1115000	271	243.0	272.3 ± 45.7**	1438000	219	152.3	132.9 ± 19.9**
	Chrysene	2225000	339	152.4		470500	12	25.5	
		638000	66	103.4		970000	72	74.2	
		1433500	202	140.9		2313000	102	44.1	
		247500	34	137.4	133.5 ± 18.2**	612000	13	21.2	41.3 ± 20.9
Lung	Control (olive oil)	310000	10	32.3		376000	14	37.2	
		296500	28	94.4		263500	11	41.7	
		646000	63	97.5		2016000	73	36.2	
		1402000	73	52.1	69.1 ± 27.8	1429000	23	16.1	32.8 ± 9.9
	1,10-DAC	1911000	539	282.1		1855000	255	137.5	
		1691000	342	202.2		1921000	151	78.6	
		1242000	430	346.2		1807000	183	101.3	
		1826500	652	357.0	296.9 ± 61.7**	2152000	281	130.6	112.0 ± 23.6**
	4,10-DAC	979500	1402	1431.3		1112000	530	476.6	
		1489000	1659	1114.2		1747000	771	441.3	
		1497000	2343	1565.1		1900000	1093	575.3	

Table 1 (*Continued*)

Tissue	Treatment	*lacZ* assay				*cII* assay			
		Individual animal data			Average ± S.D.	Individual animal data			Average ± S.D.
		No. of phages analyzed	No. of mutants	MF × 10^6	MF × 10^6	No. of phages analyzed	No. of mutants	MF × 10^6	MF × 10^6
		1673000	1702	1017.3	1282.0 ± 224.0**	1847000	1005	544.1	509.3 ± 53.0**
	Chrysene	1033000	121	117.1		1577000	61	38.7	
		1526000	371	243.1		2067000	231	111.8	
		1101000	241	218.9		1566000	115	73.4	
		871000	177	203.2	195.6 ± 47.5**	1254000	69	55.0	69.7 ± 27.2
Kidney	Control (olive oil)	447000	36	80.5		546000	21	38.5	
		741500	61	82.3		925000	23	24.9	
		1726000	62	35.9		2183000	70	32.1	
		1948000	72	37.0	58.9 ± 22.5	2244000	57	25.4	30.2 ± 5.6
	1,10-DAC	1609000	214	133.0		2570000	109	42.4	
		1510000	138	91.4		2278000	127	55.8	
		1410000	114	80.9		2621000	96	36.6	
		945000	119	125.9	107.8 ± 22.1*	1658000	67	40.4	43.8 ± 7.2*
	4,10-DAC	1378000	175	127.0		1695500	115	67.8	
		2101000	412	196.1		2526000	270	106.9	
		1447000	235	162.4		2217000	153	69.0	
		1355000	402	296.7	195.5 ± 63.3*	2014000	232	115.2	89.7 ± 21.5**
	Chrysene	1177000	161	136.8		2304000	101	43.8	
		1583000	239	151.0		2415000	157	65.0	
		1187500	241	202.9		2224000	115	51.7	
		1785000	257	144.0	158.7 ± 26.0**	2968000	147	49.5	52.5 ± 7.8**
Bone marrow	Control (olive oil)	421000	20	47.5		580000	12	20.7	
		1034000	48	46.4		1094000	25	22.9	
		1080000	61	56.5		1202000	38	31.6	
		1352000	48	35.5	46.5 ± 7.4	906000	17	18.8	23.5 ± 4.9
	1,10-DAC	1131000	78	69.0		1406000	57	40.5	
		764500	86	112.5		916000	39	42.6	
		1209000	108	89.3		1525000	58	38.0	
		732000	72	98.4	92.3 ± 15.8**	858000	48	55.9	44.3 ± 6.9**
	4,10-DAC	503500	147	292.0		779000	90	115.5	
		621000	239	384.9		1074000	191	177.8	
		1010000	200	198.0		1075000	104	96.7	
		829000	196	236.4	277.8 ± 70.2*	945000	124	131.2	130.3 ± 30.0**
	Chrysene	757500	65	85.8		1179000	20	17.0	
		819000	55	67.2		1046000	46	44.0	
		799500	49	61.3		1331000	33	24.8	
		853500	60	70.3	71.1 ± 9.1*	1392000	25	18.0	25.9 ± 10.9
Colon	Control (olive oil)	369500	17	46.0		1058000	43	40.6	
		1064000	77	72.4		1052000	40	38.0	
		660000	63	95.5		840000	36	42.9	
		676000	55	81.4	73.8 ± 18.0	1187000	33	27.8	37.3 ± 5.8
	1,10-DAC	306500	41	133.8		1715000	85	49.6	
		207000	25	120.8		1250000	57	45.6	

Table 1 (*Continued*)

Tissue	Treatment	*lacZ* assay				*cII* assay			
		Individual animal data			Average ± S.D.	Individual animal data			Average ±S.D.
		No. of phages analyzed	No. of mutants	MF × 10^6	MF × 10^6	No. of phages analyzed	No. of mutants	MF × 10^6	MF × 10^6
		988000	91	92.1		1396000	74	53.0	
		577000	75	130.0	119.2 ± 16.3*	951000	62	65.2	53.3 ± 7.3*
	4,10-DAC	469000	42	89.6		734000	48	65.4	
		369500	211	571.0		1425000	292	204.9	
		1004000	245	244.0		1089000	152	139.6	
		395000	188	475.9	345.1 ± 189.5	954000	187	196.0	151.5 ± 55.7*
	Chrysene	266500	29	108.8		980000	44	44.9	
		379000	52	137.2		1034000	68	65.8	
		1223000	222	181.5		1612000	78	48.4	
		615000	93	151.2	144.7 ± 26.2**	1178000	44	37.4	49.1 ± 10.4

Significantly different from the control group.
* $P<0.05$.
** $P<0.01$.

solution was absorbed to *E. coli* C (*lac*$^-$ *galE*$^-$) at room temperature for 20–30 min. For titration, appropriately diluted phage–*E. coli* solution was mixed with LB top agar (containing 10 mM $MgSO_4$) and plated onto dishes containing bottom agar. The remaining phage–*E. coli* solution was mixed with LB top agar containing phenyl-β-D-galactoside (3 mg/mL) and plated as described above. The mutant frequency (MF) was calculated by the following formula:

mutant frequency = (total number of plaques on selection plates/total number of plaques on titer plates) × dilution factor.

The significance of differences in the mutant frequency between the treated and control groups was analyzed by using Student's *t*-test and Welch's *t*-test in combination with the *F*-test.

2.2.4.2. cII mutant frequency determination. In the present study, we examined the mutagenicity in the lambda *cII* gene, which is also integrated as a lambda vector gene, which serves as another selective marker as reported previously in the *lacI* transgenic BigBlue mouse [24]. The positive selection for *cII* mutants was performed according to the method of Jakubczak et al. [24] with a slight modification as previously reported [9]. Briefly, the phage solution was absorbed to *E. coli* G1225 (*hfl*$^-$) at room temperature for 20–30 min. For titration, appropriately diluted phage–*E. coli* solution was mixed with LB top agar (containing 10 mM $MgSO_4$) and plated onto dishes containing bottom agar and the plates were incubated at 37 °C for 24 h. The remaining phage–*E. coli* solution was mixed with LB top agar and plated onto dishes containing bottom agar. The plates were incubated at 25 °C for 48 h for selection of *cII* mutants. The wild-type phage, recovered from Muta^{TM}Mice, has a *cI*$^-$ phenotype, which permits plaque formation with the *hfl*$^-$ strain at 37 °C but not at 25 °C. The mutant frequency was calculated by the following formula:

mutant frequency = (total number of plaques on selection plates/total number of plaques on titer plates) × dilution factor.

The significance of differences in the mutant frequency between the treated and control groups was analyzed by using Student's *t*-test and Welch's *t*-test in combination with the *F*-test.

2.2.5. Sequencing of mutants

The entire lambda *cII* region was amplified directly from mutant plaques by Taq DNA polymerase (Takara Shuzo, Tokyo, Japan) with primers P1, 5′-AAAAAGGGCATCAAATTAAACC-3′ and P2, 5′-CCGAAGTTGAGTATTTTTGCTGT-3′ as previously reported [9] (Fig. 2). A 446 bp PCR product was puri-

fied with a microspin column (Amersham Pharmacia, Tokyo, Japan) and then used for a sequencing reaction with the Ampli Taq cycle sequencing kit (PE Biosystems, Tokyo, Japan) using the primer P1. The reaction product was isolated by ethanol precipitation and analyzed with the ABI PRISM™ 310 genetic analyzer (PE Biosystems). In this study, about 40 mutants were subjected to sequence analysis in each group both in the liver and lung.

3. Results

3.1. Mutant frequencies by 1,10-DAC, 4,10-DAC and chrysene

Chrysene and its diaza-analogs, 1,10-DAC and 4,10-DAC, were tested for in vivo mutagenicity using *lacZ* transgenic mice (Muta™Mice). Chrysene and 4,10-DAC were injected at the total dose of 800 mg/kg

Table 2
Sequences of *cII* mutations in the liver of 1,10-DAC-treated Muta™Mouse

Mutant no.	Position	Mutation	Sequence			Amino acid change
C1	117	G to T	TCG	CAG	ATC	Gln to His
C2	42	G to T	ATC	GAG	AGT	Glu to Asp
C3	126	G to T	AGC	AGG	TGG	Arg to Ser
C4	40–43	−GA	GAG	AGT	GCG	Frameshift
C5	166	G to T	CTT	GCT	GTT	Ala to Ser
C6	233	T to A	ATT	CTC	ACC	Leu to His
C7	132	G to T	TGG	AAG	AGG	Lys to Asn
C8	89	C to T	ACA	GCG	GAA	Ala to Val
C9	11	C to TA	CGT	GCA	AAC	Frameshift
C10	178	T to A	GAA	TGG	GGG	Trp to Arg
C11	197	A to G	GAC	GAC	ATG	Asp to Gly
C12	179	G to T	GAA	TGG	GGG	Trp to Leu
C13	29	C to A	GAG	GCT	CTA	Ala to Asp
C14	101	G to T	GTG	GGC	GTT	Gly to Val
C15	89	C to T	ACA	GCG	GAA	Ala to Val
C16	117	G to C	TCG	CAG	ATC	Gln to His
C17	40	G to A	ATC	GAG	AGT	Glu to Lys
C18	294	A to C	TTC	TGA	–	Stop to Cys
C19	150	G to T	CCA	AAG	TTC	Lys to Asn
C20[a]	294	A to C	TTC	TGA	–	Stop to Cys
C21	211	G to A	TTG	GCG	CGA	Ala to Thr
C22	111	G to T	GAT	AAG	TCG	Lys to Asn
C23	123	C to A	ATC	AGC	AGG	Ser to Arg
C24	160	C to A	ATG	CTG	CTT	Leu to Met
C25	173	T to C	GTT	CTT	GAA	Leu to Pro
C26	125	G to C	AGC	AGG	TGG	Arg to Thr
C27	−3	C to G	tta	cat	ATG	Base substitution in the 5′-flanking region
C28	29	C to A	GAG	GCT	CTA	Ala to Asp
C29[a]	111	G to T	GAT	AAG	TCG	Lys to Asn
C30	38	T to A	CGA	ATC	GAG	Ile to Asn
C31	40	G to T	ATC	GAG	AGT	Glu to Stop
C32	163	C to T	CTG	CTT	GCT	Leu to Phe
C33	79	G to T	ACT	GAG	AAG	Glu to Stop
C34	57	C to A	CTT	AAC	AAA	Asn to Lys
C35	89	C to T	ACA	GCG	GAA	Ala to Val
C36	179–184	−G	TGG	GGG	GTC	Frameshift
C37	113	C to A	AAG	TCG	CAG	Ser to Stop
C38	89	C to G	ACA	GCG	GAA	Ala to Gly
C39	123	C to G	ATC	AGC	AGG	Ser to Arg
C40	125	G to A	AGC	AGG	TGG	Arg to Lys

[a] Ascribable to the same mutation obtained in an identical mouse.